PFC/RR-86-2

DOE/ET-51013-173
UC-20, a, d, f

Circular Waveguide Mode Converters at 140 GHz

J. Trulsen*; P. Woskoboinikow; R. J. Temkin

January 1986

Plasma Fusion Center
Massachusetts Institute of Technology
Cambridge, MA 02139 USA

*Present Address: Institute of Mathematical and Physical Sciences
University of Tromso
N-9001 Tromso, Norway

ABSTRACT

A unified derivation of the coupled mode equations for circular waveguide is presented. Also, approximate design criteria for TE_{0n} - to - TE_{0n} axisymmetric, TE_{01} - to - TE_{11} wriggle, and TE_{01} - to - TM_{11} bend converters are reviewed. Numerically solving the coupled mode equations, an optimized set of mode converters has been designed for conversion of a 2 millimeter wave TE_{03} mode into TE_{11}. This set consists of axisymmetric TE_{03} - to - TE_{02} and TE_{02} - to - TE_{01} converters followed by a wriggle TE_{01} - to - TE_{11} converter. This mode converter set was fabricated and tested using a 3 kW, 137 GHz gyrotron. A TE_{11} mode purity of better than 97% was achieved. The TE_{01} - to - TE_{11} wriggle converter was experimentally optimized for a measured conversion efficiency of better than 99% not including ohmic losses.

I. INTRODUCTION

The damping rate of the TE_{01} mode in a circular waveguide decreases inversely proportional to increasing waveguide radius and the three halves power of the wave frequency. This means that low-loss communication systems in the microwave frequency range are possible using oversized circular waveguides for transmission. This observation initiated a major research effort, particularly at Bell Laboratories during the 1950's and 1960's (Miller (1954), Schelkunoff (1955), Morgan (1957), Unger (1958), Rowe and Warters (1962)). One of the key points for this research was the unwanted conversion of microwave power from the TE_{01} mode into more heavily damped modes due to imperfections in the circular guide, guide bends and so one. The development of the optical fiber in the 1970's, however, eventually led to a vaning interest in the above scheme.

With the development of high-power (200 kW) gyrotrons in the 28 - 70 GHz range for electron cyclotron resonance heating (ECRH) applications in plasma fusion devices interest in overmoded circular waveguides is again increasing. The large cross section now being required mainly due to the necessity of transporting high power levels down the guide without electrical breakdowns. Mode conversion is now not necessarily an unwanted effect. Depending on the specific design and mode of operation, gyrotrons produce most of their energy in the TE_{02}, TE_{03} or even higher order modes. These modes are not optimal for being launched directly into the plasma as regards polarization or radiation pattern. Thus several different schemes have been developed for transforming the generated power into the TE_{01} mode for the propagation from the gyrotron to the plasma device and

then subsequently into better suited modes for launching into the plasma, making use of controlled perturbations of the waveguide wall (Doane (1982) and (1985), Moeller (1982), Thumm et al. (1984)). Other approaches combine the use of circular waveguides with quasi-optical methods (Vlasov and Orlova (1974), Wengenroth (1978), Gallagher and Sweeney (1983)).

With the recent development of high power gyrotrons in the 140 GHz range and above (Kreischer, et al., 1984) a reassessment of the possibilities of using overmoded circular waveguides for radiation transport and mode conversion is necessary. Key issues in this connection are conversion efficiencies, mode control and the mechanical requirements during manufacturing and operation of the waveguide system imposed by the small wavelengths in this frequency range. The following study is related to the 140 GHz scattering diagnostic system being developed for the plugs of the TARA tandem mirror experiment. The gyrotron will deliver about 1 kW in long pulse (30 - 100ms) operation. More than 99% of the power from the gyrotron will appear in the circular TE_{03} mode as will be shown in Section V.

In the following section a unified derivation of the coupled mode equations for the deformed circular guide are presented. Simplified design criteria are given in Section III. Section IV contains numerical results on converter optimalization for the TE_{03} 140 GHz gyrotron. Section V will contain the experimental verifications of operation of the designed waveguide system. Finally, Section VI will summarize this work.

II. COUPLED MODE EQUATIONS

The electric and magnetic fields $\underline{E}$ and $\underline{H}$, with time dependence $e^{j\omega t}$, which exist in the perturbed waveguide satisfy Maxwell's equations

$$\nabla \times \underline{E} = - j \omega \mu \underline{H} \tag{1}$$

$$\nabla \times \underline{H} = j \omega \epsilon \underline{E} \tag{2}$$

In the following we shall derive coupled mode equations for the fields inside a generally curved waveguide of varying circular or deformed cross section. For this purpose it will be convenient to introduce local toroidal coordinates (r, ϕ, w) where r and ϕ are polar coordinates centered on the axis of the torus and w is the arclength along this axis. The local section of the waveguide wall will be given by

$$r = a (w) + \rho (\phi, w) \tag{3}$$

where it will be assumed that

$$\int_0^{2\pi} d\phi \; \rho (\phi, w) = 0 \tag{4}$$

With $\underline{e}$ and $\underline{h}$ being the normalized perpendicular wave fields of a particular mode in the locally embedded perfectly conducting straight circular (ideal) guide (for notation used in the subsequent discussion see Appendix A) the following identity will be useful

$$\underline{h} \cdot \nabla \times \underline{E} = \nabla \cdot (\underline{E} \cdot \underline{e} \, \hat{\underline{w}}) - \nabla \cdot (E_w \underline{e}) + \underline{E} \cdot \nabla \times \underline{h} \tag{5}$$

Since

$$\nabla \cdot (\underline{E} \cdot \underline{e} \, \hat{\underline{w}}) = \frac{1}{1 + \xi} \frac{\partial}{\partial w} (\underline{E} \cdot \underline{e})$$

$$\hat{\underline{w}} \cdot \nabla \times \underline{h} = \delta^e p^2 \Phi$$

$$(1 + \xi) (\nabla \times \underline{h})_\perp = \frac{da}{dw} \frac{\partial}{\partial a} \underline{e}$$

and using

$$E_w = \frac{\hat{w}}{j\omega\epsilon} \cdot \nabla \times \underline{H}$$

the identity (5) can be written in the form

$$(1 + \xi)\, \underline{h} \cdot \nabla \times \underline{E} = \frac{\partial}{\partial w} (\underline{E} \cdot \underline{e}) - (1 + \xi)\, \nabla \cdot (E_w \underline{e}) + \frac{da}{dw}\, \underline{E} \cdot \frac{\partial}{\partial a}\, \underline{e}$$

$$+ \delta^e\, p^2\, \Phi\, \xi\, E_w + \hat{w} \cdot \nabla \times (\delta^e \frac{p^2}{j\omega\epsilon}\, \Phi\, \underline{H}) - \delta^e \frac{p^2}{j\omega\epsilon}\, \underline{H} \cdot \underline{h} \qquad (6)$$

For the last term of (6) we assumed ϵ to be constant over the cross section of the guide. A similar calculation, this time assuming μ to be constant, leads to

$$-(1 + \xi)\, \underline{e} \cdot \nabla \times H = \frac{\partial}{\partial w} (\underline{H} \cdot \underline{h}) - (1 + \xi)\, \nabla \cdot (H_w \underline{h}) - \frac{da}{dw}\, \underline{H} \cdot \frac{\partial}{\partial a}\, \underline{h}$$

$$+ \delta^h\, p^2\, \Phi\, H_w - \hat{w} \cdot \nabla \times (\delta^h \frac{p^2}{j\omega\mu}\, \Phi\, \underline{E}) + \delta^h \frac{p^2}{j\omega\mu}\, \underline{E} \cdot \underline{e} \qquad (7)$$

In the above formulas

$$\xi = \frac{r}{b} \cos(\phi - \phi_0)$$

where b is the local radius of curvature of the toroidal axis, ϕ_0 defines the osculating plane of the toroidal axis and

$$\delta^e = 1 \qquad \delta^h = 0 \qquad \text{for TM - modes}$$

$$\delta^e = 0 \qquad \delta^h = 1 \qquad \text{for TE - modes.}$$

The remaining quantities are defined in Appendix A.

We now define

$$V(w) = \int \underline{E} \cdot \underline{e}\, dS$$

$$I(w) = \int \underline{H} \cdot \underline{h}\, dS \tag{8}$$

where the integration is extended over the cross section of the locally embedded ideal guide. If necessary the fields of the perturbed guide are extrapolated to the same cross section.

Operating on (1) and (2) with the operators $\int dS(1+\zeta)\underline{h}\,\cdot$ and $\int dS(1+\zeta)\underline{e}\,\cdot$ respectively, using the identities (6) and (7) we now find

$$\dot{V} + (j\omega\mu + \delta^e \frac{p^2}{j\omega\epsilon})I = a\oint d\phi(1+\zeta)\, E_w\, \underline{e} \cdot \hat{\underline{r}}$$

$$- \int dS\, \zeta\, (j\omega\mu\, \underline{H} \cdot \underline{h} + \delta^e\, p^2\, \Phi\, E_w) - \frac{da}{dw}\left[\int dS \underline{E} \cdot \frac{\partial}{\partial a}\underline{e} - a\oint d\phi\, \underline{E} \cdot \underline{e}\right] \tag{9}$$

$$\dot{I} + (j\omega c + \delta^h \frac{p^2}{j\omega\mu}) V = \delta^h \frac{p^2}{j\omega\mu} a\oint d\phi\, E_\phi \Phi$$

$$-\int dS\xi (j\omega c \underline{E} \cdot \underline{e} + \delta^h p^2 \Phi H_w) - \frac{da}{dw}\left[\int dS \underline{H} \cdot \frac{\partial}{\partial a} \underline{h} - a\oint d\phi\, \underline{H} \cdot \underline{h}\right]$$

where the dots indicate derivation with respect to w, $\dot{V} = \frac{d}{dw} V$ and $\dot{I} = \frac{d}{dw} I$.

Apart from the possible extension of integrals to the locally embedded ideal guide cross section, equations (9) are exact integral relations satisfied by the fields $\underline{E}$ and $\underline{H}$. In particular, with $\xi = \frac{da}{dw} = 0$ and $E_w = E_\phi = 0$ at the wall, these equations reduce to the well-known generalized telegraphist equations of non-interacting wavemodes in the ideal guide (see appendix A). The derivation of coupled mode equations now rests on finding suitable approximations for the right hand side integrals. To this end the fields in the perturbed guide are next decomposed as

$$\underline{E} = \underline{E}_0 + \underline{E}_1 \qquad \underline{H} = \underline{H}_0 + \underline{H}_1$$

where

$$\underline{E}_0 = \sum V\underline{e} + \sum \delta^e \frac{p^2}{j\omega c} I \Phi \hat{\underline{w}} \qquad (10)$$

$$\underline{H}_0 = \sum I \underline{h} + \sum \delta^h \frac{p^2}{j\omega\mu} V \Phi \hat{\underline{w}}$$

The summations are carried over all modes of the locally embedded ideal guide.

Our basic assumption is now that $\underline{E}_1$ and $\underline{H}_1$ are small and localized to the wall region. We therefore neglect the contribution from $\underline{E}_1$ and $\underline{H}_1$ to integrals extended over the cross section of the locally embedded ideal guide. Making use of the identities

$$\underline{e}_s \cdot \underline{e}_{s'} = \underline{h}_s \cdot \underline{h}_{s'}$$

$$\underline{e}_{s'} \cdot \frac{\partial}{\partial a} \underline{e}_s = \underline{h}_{s'} \cdot \frac{\partial}{\partial a} \underline{h}_s$$

the result is

$$\dot{V}_s + (j\omega\mu + \delta_s^e \frac{p_s^2}{j\omega\epsilon}) I_s = a \oint d\phi \, (1 + \xi) E_{1w} \underline{e}_s \cdot \hat{\underline{r}}$$

$$- \sum_{s'} (j\omega\mu G_{ss'} + \delta_s^e \delta_{s'}^e \frac{p_s^2 p_{s'}^2}{j\omega\epsilon} g_{ss'}) I_{s'} - \sum_{s'} K_{ss'} V_{s'}$$

(11)

$$\dot{I}_s + (j\omega c + \delta_s^h \frac{p_s^2}{j\omega\mu}) V_s = \delta_s^h \frac{p_s^2}{j\omega\mu} a \oint d\phi \, E_{1\phi} \Phi_s$$

$$- \sum_{s'} (j\omega c \, G_{ss'} + \delta_s^h \delta_{s'}^h \frac{p_s^2 p_{s'}^2}{j\omega\mu} g_{ss'}) V_{s'} - \sum_{s'} K_{ss'} I_{s'}$$

where

$$G_{ss'} = \int dS \, \xi \, \underline{e}_{s'} \cdot \underline{e}_s$$

$$g_{ss'} = \int dS \, \xi \, \phi_{s'} \phi_s \qquad (12)$$

$$K_{ss'} = \frac{da}{dw} \left[dS \, \underline{e}_{s'} \cdot \frac{\partial}{\partial a} \underline{e}_{s'} - a \oint d\phi \, \underline{e}_s \cdot \underline{e}_s \right]$$

It is seen that the G and g coefficients are symmetric with respect to mode indices.

The usefulness of the general coupled mode equations is easily demonstrated by considering some important special cases.

i) For the perfectly conducting straight guide of varying circular cross section $\xi = \rho = 0$ while $E_{1\phi} = 0$ at the wall. The coupling coefficients K are non-vanishing only for mode pairs m,n and m',n'

satisfying $m = m'$. The TE_{on} - modes couple only among themselves, they satisfy the boundary conditions for the fields at the perturbed wall since $\underline{e} = 0$ here and

$$K_{[on][on']} = \begin{cases} \frac{2}{a}\frac{da}{dw}\frac{\chi_{[on]}\ \chi_{[on']}}{\chi_{[on']}^2 - \chi_{[on]}^2} & n' \neq n \\ 0 & n' = n \end{cases} \qquad (13)$$

where $\chi_{[on]}$ is the nth zero of the Bessel function derivative J_o'.

This result is in accordance with Unger's (1958) classical result.

The other cylindrical waveguide modes do not satisfy the boundary conditions for the fields at the perturbed wall. This requires the substitution

$$E_{lw} = -\frac{da}{dw}\ E_{or}$$

in the wall contribution term of (11) and the line integral part of the coupling coefficients K will no longer vanish. The validity of the resulting coupled mode equations requires da/dw to be small.

ii) For the perfectly conducting circular cross section bend $\frac{da}{dw} = 0$ while $E_{l\phi} = E_{lw} = 0$ at the wall. The coupling coefficients G and g are non-vanishing only for mode pairs m,n and m′,n′ satisfying $|m - m'| = 1$ in accordance with Morgan's (1957) classical result. The explicit

evaluation of the coupling coefficients generally seems to require numerical methods. Analytic results are, however, known for a few cases. Thus

$$g_{(on)(1n')} = G_{(on)(1n')} = G_{(on)[1n']} = 0$$

$$g_{[on][1n']} = \frac{\sqrt{2a}}{b} \frac{x_{[1n']}(x^2_{[on]} + x^2_{[1n']})}{(x^2_{[1n']} - 1)^{1/2}(x^2_{[on]} - x^2_{[1n']})^2}$$

$$G_{[on](1n')} = \frac{a}{\sqrt{2}b} \frac{1}{x_{[on]}} \delta_{n,n'} \qquad (14)$$

$$G_{[on][1n']} = \frac{2\sqrt{2a}}{b} \frac{x^2_{[on]}\, x_{[1n']}}{(x^2_{[1n']} - 1)^{1/2}\,(x^2_{[on]} - x^2_{[1n']})^2}$$

$$G_{[2n](1n')} = \frac{2a}{b} \frac{1}{(x^2_{[2n]} - 4)^{1/2}(x^2_{[1n']} - x^2_{[2n]})}$$

iii) For the perfectly conducting, straight but deformed guide $\xi = \frac{da}{dw} = 0$. The boundary condition for the electric field at the actual wall, $\underline{n} \times \underline{E} = 0$, can now be replaced by the approximate expression

$$\left(\hat{\underline{r}} - \frac{1}{r}\,\frac{\partial \rho}{\partial \phi}\,\hat{\underline{\phi}} - \frac{\partial \rho}{\partial w}\,\hat{\underline{w}}\right) \times \left(\underline{E}_0 + \rho\,\frac{\partial}{\partial r}\,\underline{E}_0 + \underline{E}_1\right) = 0$$

where $\underline{E}_0$ and $\underline{E}_1$ are both evaluated at r = a. Thus to lowest order

$$E_{1\phi} = -\rho\,\frac{\partial}{\partial r}\,E_{0\phi} - \frac{1}{r}\,\frac{\partial \rho}{\partial \phi}\,E_{0r}$$

$$E_{1w} = -\rho\,\frac{\partial}{\partial r}\,E_{0w} - \frac{\partial \rho}{\partial w}\,E_{0r}.$$

Choosing the wall perturbation to be of the form

$$\rho\,(\phi, w) = d \sin\,(\lambda\phi - \kappa w)$$

it is seen from (11) and (12) that the coupling coefficients are non-vanishing only for mode pairs m,n and m′,n′ of similar polarization satisfying $|m - m'| = \lambda$ or $m + m' = \lambda$. The derivation of analytic expressions for the coupling coefficients is straightforward, if tedious, and will be omitted.

iv) For the straight circular guide with a wall of finite conductivity $\xi = \frac{da}{dw} = 0$ while at the wall

$$\underline{E}_1 = \frac{1+j}{\sigma\delta}\,\underline{H}_0 \times \hat{\underline{r}}$$

Here σ and $\delta = \sqrt{\frac{2}{\omega\mu\sigma}}$ are the wall conductivity and skin depth, respectively. Substitution into (11) leads to the well-known expression for the damping coefficients of the different modes (Collin, 1966)

$$\alpha_{mn} = \frac{1}{a\sigma\delta}\sqrt{\frac{\epsilon}{\mu}}\left(1 - \frac{p_{mn}^2}{\omega^2\epsilon\mu}\right)^{-1}\left(\delta^e + \delta^h\left(\frac{p_{mn}^2}{\omega^2\epsilon\mu} + \frac{m^2}{\chi_{mn}^2 - m^2}\right)\right) .$$

In addition, the finite conductivity of the wall also induces coupling between modes m,n and m',n' of similar polarizations satisfying $m = m'$. The derivation of analytic expressions for the coupling coefficients is again straightforward and will be omitted.

The I and V variables of the generalized telegraphist equations (11) contain both forward and backward propagating waves. Separation between the different directions of propagations is achieved by introducing the amplitudes A and R for the advancing and reflected waves according to

$$V = \sqrt{Z}\,(A + R)$$

$$I = \frac{1}{\sqrt{Z}}(A - R) \qquad (15)$$

where Z is the wave impedance of the mode in choice (see appendix A). Note that the amplitudes A and R here include rapidly varying phase factors. The general equations for the amplitudes are

$$\dot{A}_s + i\beta_s A_s + \frac{\dot{Z}_s}{2Z_s} R_s = \frac{a}{2\sqrt{Z_s}} \oint d\phi\, (1+\xi)\, E_{1w}\, \underline{e}_s \cdot \hat{\underline{r}} + \frac{a}{2} \sqrt{Z_s}\, \delta_s^h \frac{p_s^2}{j\omega\mu}$$

$$\oint d\phi\, E_{1\phi} \Phi_s - \sum_{s'} j\,(\gamma^+_{ss'} A_{s'} - \gamma^-_{ss'} R_{s'}) - \sum_{s'} (\kappa^+_{ss'} A_{s'} + \kappa^-_{ss'} R_{s'})$$

(16)

$$\dot{R}_s - i\beta_s R_s + \frac{\dot{Z}_s}{2Z_s} A_s = \frac{a}{2\sqrt{Z_s}} \oint d\phi\, (1+\xi)\, E_{1w}\, \underline{e}_s \cdot \hat{\underline{r}} - \frac{a}{2} \sqrt{Z_s}\, \delta_s^h \frac{p_s^2}{j\omega\mu}$$

$$\oint d\phi\, E_{1\phi} \Phi_s - \sum_{s'} j\,(\gamma^-_{ss'} A_{s'} - \gamma^+_{ss'} R_{s'}) - \sum_{s'} (\kappa^-_{ss'} A_{s'} + \kappa^+_{ss'} R_{s'})$$

with

$$\beta_s = (\omega^2 \epsilon\mu - p^2)^{1/2}$$

$$\gamma^+_{ss'} = \frac{1}{2} \left(\frac{j\omega\mu}{\sqrt{Z_s Z_{s'}}} + j\omega\epsilon \sqrt{Z_s Z_{s'}} \right) G_{ss'} + \frac{1}{2} \left(\delta_s^e \delta_{s'}^e \frac{p_s^2 p_{s'}^2}{\sqrt{Z_s Z_{s'}}} \right.$$

$$\left. + \delta_s^h \delta_{s'}^h \frac{p_s^2 p_{s'}^2}{j\omega\mu} \sqrt{Z_s Z_{s'}} \right) g_{ss'}$$

$$\kappa^{\pm}_{ss'} = \frac{1}{2} K_{ss'} \left(\frac{Z_{s'}}{Z_s} \pm \frac{Z_s}{Z_s} \right) \qquad (17)$$

It is seen that for modes far from cut-off the coupling between advancing and reflected waves is much smaller than the coupling between advancing waves only. This observation often makes it possible to neglect reflected waves all together and only consider the advancing waves.

III. APPROXIMATE DESIGN CRITERIA

The problem of designing efficient mode converters for given pairs of propagating modes with propagation parameters β_1 and β_2 is now reduced to finding the proper wall perturbation. For non-degenerate mode pairs, $\beta_1 \neq \beta_2$, this normally means choosing a periodicity of the perturbation corresponding to the beat wavelength L, of the given mode pair, $L = 2\pi/|\beta_1 - \beta_2|$. For the highly overmoded guide, approximations for the remaining parameters can often be found by neglecting effects of reflected and non-propagating modes in the coupled mode equations (Moeller (1982)). Generally we are seeking approximate equations for the part of Q_s defined by

$$A_s = Q_s \, e^{-j\beta_s z}$$

varying slowly over the beat wavelength L. In the following we consider a few important cases.

i) For the TE_{on} to TE_{on}, axisymmetric ripple converter

$$a(z) = a\,(1 + \eta \sin(\tfrac{2\pi}{L} z)) \tag{18}$$

the coupled mode equations (16) reduce to

$$\frac{d}{dz} A_1 + i\beta_1 A_1 = - \frac{2\pi}{L} K\eta \cos\left(\frac{2\pi}{L} z \right) \quad A_2$$

$$\frac{d}{dz} A_2 + i\beta_2 A_2 = \quad \frac{2\pi}{L} K\eta \cos\left(\frac{2\pi}{L} z \right) A_1$$

with

$$K = \frac{2 \chi_1 \chi_2}{\chi_2^2 - \chi_1^2} \quad .$$

The slowly varying part of the Q's thus satisfy

$$\frac{d}{dz} Q_1 = - \frac{\pi}{L} K \eta Q_2$$

(19)

$$\frac{d}{dz} Q_2 = \frac{\pi}{L} K \eta Q_1$$

Conversion from mode 1 to mode 2 is achieved if the relative ripple amplitude η and the converter length ℓ satisfy the condition

$$\frac{\pi}{L} K \ell \eta = \frac{\pi}{2} \quad .$$

Expressing the converter length in units of the beat wavelength, $\ell = NL$, this condition can be written in the form

$$N\eta = \frac{1}{2K} \tag{20}$$

ii) For the TE_{01} to TE_{11} wriggle converter with a deformation of the converter axis of the form

$$y = a\eta \sin\left(\frac{2\pi}{L} z\right) \tag{21}$$

the analysis is rather similar. For small wriggle amplitudes the curvature of the axis can be approximated as

$$\frac{1}{b} = -\left(\frac{2\pi}{L}\right)^2 a\eta \sin\left(\frac{2\pi}{L}\right)z.$$

The coupled mode equations (16) thus reduce to

$$\frac{d}{dz} A_1 + j\beta_1 A_1 = -j \frac{2\pi}{L} K \eta \sin\left(\frac{2\pi}{L}z\right) A_2$$

$$\frac{d}{dz} A_2 + j\beta_2 A_2 = -j \frac{2\pi}{L} K \eta \sin\left(\frac{2\pi}{L} z\right) A_1$$

The explicit expression for the constant K is this time found by substituting the appropriate expressions for G and g from (14) into (17). The slowly varying part of the Q's again satisfy equations (19), leading to the previous condition for mode conversion (20) (but with a different expression for K).

The beat wavelength in the highly overmoded guide can be approximated as

$$L \approx \frac{4\pi a^2}{c} \frac{1}{|\chi_2^2 - \chi_1^2|} \quad . \tag{22}$$

Thus, in the above examples the choice of a particular perturbation wavelength L essentially determines at what frequency the converter will operate. The total length of the converter and the relative perturbation amplitude will then have to be adjusted to achieve the optimal conversion efficiency. The relative frequency bandwidth $\frac{\Delta\omega}{\omega}$ of the converter, on the other hand, varies inversely with the length of the converter (Moeller (1982)).

iii) For degenerate mode pairs, $\beta_1 = \beta_2$, the analysis can be simplified even further. Thus, for the constant curvature TE_{01} to TM_{11} converter (Doane (1982)) the coupled mode equations (16) reduce to

$$\frac{d}{dz} A_1 + i\beta A_1 = -j K A_2$$

$$\frac{d}{dz} A_2 + i\beta A_2 = -j K A_1$$

with

$$K = \frac{a}{\sqrt{2}b} \frac{\omega}{c} \frac{1}{\chi_{[01]}} .$$

Complete conversion requires a converter length ℓ satisfying

$$K\ell = \frac{\pi}{2} ,$$

or expressed in terms of the total angular deviation θ of the converter

$$\theta = \frac{\ell}{b} = \frac{\chi_{[01]} \pi c}{\sqrt{2}\, \omega\, a} \qquad (23)$$

The above approximate formulas (18) - (23) often represent good first guesses to parameters of a particular converter design problem provided the beat wavelength for the two modes of interest does not fall too close to the beat wavelength for other mode pairs. Optimalization of the converter parameters will, however, require the numerical solution of the coupled mode equations (16) for a sufficiently large collection of modes. In particular the conversion efficiency of the converter will depend on the participation of non-wanted modes in the conversion process. Part of the available wave power will oscillate between these modes throughout the length of the converter. The ultimate conversion efficiency depends on the amplitude and the phase of these oscillations at the end of the converter. These amplitudes and phases can partly be controlled by the choice of converter length, converter diameter or the detailed form of the perturbation of the waveguide wall.

IV. OPTIMIZED CONVERTER DESIGNS

A set of circular waveguide mode converters for conversion of a 2mm wave TE_{03} mode into a TE_{11} mode have been designed. These designs were accomplished by using the approximations of Section 3 to make initial guesses of the mode converter parameters and then optimizing these parameters by numerical solution of equation (16) for up to five modes with reflections neglected.

It was first found by numerical calculations that it did not seem feasible to make an efficient waveguide converter for a direct conversion between the TE_{03} and TE_{01} modes. The principal reason for this was that the beat wavelengths for the mode pairs $TE_{03} - TE_{01}$ and $TE_{03} - TE_{04}$ fall too close together. Even by reducing the converter diameter close to or below the cut-off for the TE_{04} mode the interaction with the TE_{02} mode is too strong. At the same time the necessary perturbation wavelength L becomes comparable to the free space wavelength.

A pair of mode converters, TE_{03} - to - TE_{02} and TE_{02} - to - TE_{01} can, however, be made compact and with efficiencies close to 100%. For the given frequency range a waveguide diameter close to 1.27cm (0.5 inch) seems to be optimal for both converters as regards competition with unwanted modes. The dimension of the gyrotron output guide was therefore chosen to be exactly 0.5 inch, coincident with the maximum diameter of the rippled mode converters. For both converters the waveguide radius, as illustrated in Fig. 1a, varies as

$$r = a\left(1 - \nu + \nu \cos\left(\frac{2\pi}{L} z\right)\right)$$

for z in the interval 0 to $\ell = NL$, where N is an integer number. In particular, smooth transitions between the converters and the adjoining waveguides are achieved without tapers.

The optimized parameters and the corresponding theoretical efficiencies of these converters are listed in Table I. The center frequency for these designs is 137 GHz. A change in the pertubation wavelength, L, by 1% changes the center frequency by approximately 1 GHz. For example, increasing the TE_{03} - to - TE_{02} beat wavelength from 2.148 to 2.210cm and the TE_{02} - to - TE_{01} beat wavelength from 3.50 to 3.59cm will center these mode converters at a frequency of 140 GHz (this has been confirmed by numerical calculations). Also if the perturbation wavelength, L, is held constant, a 1% change in the mode converter radius, a, will change the center frequency approximatley 2.5 GHz.

Figures 2a and 3a depict the computed power oscillations between different modes throughout the converter length at the design frequency. The corresponding frequency dependence of the two converter efficiencies are given in Figs. 2b and 3b. The 90% conversion bandwidth for the TE_{03} - to - TE_{02} converter is about 6 GHz and for the TE_{02} - to - TE_{01} converter about 7 GHz.

With total lengths of 107mm and 175mm the TE_{03} - to - TE_{02} and TE_{02} - to - TE_{01} converters are so compact that they can be easily fitted within the gyrotron vacuum system. Their power handling capabilities thus far exceeds the present requirements for up to 10kW. Going to smaller guide diameters and therefore even more compact designs, however, seems to lead to reduced converter efficiencies.

Several options are available for the subsequent part of the waveguide system. Combining a Vlasov coupler (Vlasov and Orlova (1974)) with optical filtering methods will produce a linearly polarized near-Gaussian beam. This approach leads to compact designs, however, a large amount of filtering would be required to produce a circularly symmetric beam significantly

compromising efficiency. Another approach is to use a smooth circular waveguide bend to convert from the TE_{01} mode to the degenerate TM_{11} mode followed by a corrugated converter into the HE_{11} mode (Doane (1982)). We will be converting the TE_{01} mode into the nearly linearly polarized TE_{11} mode using a wriggler converter (Moeller (1982)) followed by a corrugated TE_{11} to HE_{11} converter with a decreasing corrugation depth from $\lambda/2$ to $\lambda/4$ (Thumm (1985)). This approach has lower ohmic losses than conversion via the TM_{11} mode.

The chosen TE_{01} - to - TE_{11} converter design with an axial deformation

$$x = 0,\ y = a\ \nu\ \sin(\frac{2\pi}{L})z$$

for z in the interval 0 to $\ell = NL$, where N is not necessarily an integer in this case, is depicted in Fig. 1b. This form for the converter axial deformation was chosen so that there would be no sharp discontinuity in the waveguide radius of curvature between the input straight waveguide and mode converter. Optimized parameters for the 0.5 inch diameter design are summarized in Table II. The power oscillations between different modes throughout the converter length are shown in Fig. 4a. Even with relatively large number of beat wavelengths the frequency bandwidth of this converter is reasonable. As shown in Fig. 4b, the 90% conversion bandwidth is about 4.5 GHz. This converter introduces a finite angular deviation (~1°) of the waveguide system because the length of this converter is a non-integral number of perturbation wavelengths. Even so conversion into the TM_{11} - mode does not represent a problem. As seen from Fig. 4a the finite deviation angle is dictated by the need to terminate the mode converter at a length that minimizes the contribution from the TE_{21} - mode at the output.

The theoretical conversion efficiency is increased by approximately 1% by letting the relative wriggle amplitude ν increase linearly with distance from $\nu = 0.041$ to $\nu = 0.085$ along the length of the converter. This change reduces the amplitude of the TE_{12} oscillation while the amplitude of the TE_{21} oscillation increases slightly. A more complicated variation of wriggle amplitude along the length of the converter can further improve the conversion efficiency as will be shown in the next section. If converter length is a critical issue a more compact design with similar efficiency results by reducing the converter diameter. A 8mm diameter design is also included in Table II. For both designs the power loss due to finite conductivity is of the order of 2%. The larger diameter design was chosen. While it is still of moderate length it avoids the use of down tapers and therefore reduces the possibility of trapped radiation.

The 137 GHz center frequency of the chosen TE_{01} - to - TE_{11} converter design is sensitive to small changes in the perturbation wavelength or waveguide diameter. A 1% change in perturbation wavelength changes the center frequency approximately 1.2 GHz. Increasing the perturbation wavelength from 12.90 to 13.21cm will center this converter at 140 GHz. This converter, as the axisymmetric converters, is more sensitive to small changes in waveguide diameter. A 1% change in waveguide diameter changes the center frequency approximately 3 GHz (increasing diameter corresponding to increasing center frequency).

The purpose of the final part of the waveguide system, a corrugated guide, is to provide for suppression of sidelobes and improved polarization of the launched beam. Converting to the HE_{11} - mode by corrugated guide is well known at lower frequencies (James (1981) Doane, (1982), Thumm (1984)).

We will be fabricating such a converter with a period of $\lambda/3$ and linearly varying slot depth from $\lambda/2$ to $\lambda/4$ over a length of 38cm. Work at lower frequencies (Thumm (1985)) suggests that such a converter will have a conversion efficiency of greater than 20dB.

V. EXPERIMENTAL RESULTS

A. Axisymmetric Converters

The axisymmetric mode converters, with the dimensions given in Table I, were fabricated by electroforming copper onto an aluminum mandrel and then dissolving the aluminum.

The mode converters were tested by using the circular guide TE_{03} output from a gyrotron. Output power was approximately 3kW in short 1.5μs pulses, pulsed 4 times a second. The mode purity at each stage of conversion was estimated by far field pattern measurements which were compared to calculated radiation patterns using the equations of Rissler (Silver (1949)).

The measurements were made using either a Hughes or Aerowave 110-170 GHz band detector diode. On the front end of the detector diode there was a 24dB gain horn, frequency meter, and calibrated 0-50dB attenuator, all from Hughes. The detection system was swung on a horizontal arc with the detection horn 41cm from the waveguide or converter being tested. This satisfied the rule for far field measurement, $R > 4a^2/\lambda$, by a large margin.

As the detection system was swung through the radiation pattern peaks and valleys the calibrated attenuator was adjusted to keep the diode signal constant. The change in attenuator setting relative to the maximum radiation peak was then plotted to give the far field pattern. The frequency meter was used to periodically check that the gyrotron TE_{03} mode was always being measured.

A Scientec calorimeter was used for absolute and relative power measurements. Relative power measurements between the input and output of the converters tested showed no power losses within an accuracy of about $\pm 5\%$.

The gyrotron TE_{03} mode frequency was 137.28 GHz for these initial axisymmetric mode converter tests. The unconverted gyrotron output launched through a 3λ thick fused quartz vacuum window is shown in Fig. 5a. The agreement between the measured points and calculated curve is excellent for a circular guide TE_{03} mode.

The TE_{03} - to - TE_{02} mode converter was butted up to the gyrotron vacuum window and the resulting far field pattern is shown by the points in Fig. 5b. The solid curve in that figure was calculated for a circular guide TE_{02} mode. The agreement between measurement and theory is only fair. More reasonable agreement with a calculated far field pattern is achieved if it is assumed that 20% of the radiation energy is in the TE_{03} mode 180° out of phase with the TE_{02} mode. (The relative phase between modes determines the angular position of the higher order peaks.) The modification to the far field pattern for this situation is shown by the dashed curves in Fig. 5b.

An 80% conversion efficiency for this converter is much poorer than predicted in Table I. This discrepancy could be attributable to imperfections in the converter or to the 3λ gap and window between the gyrotron output waveguide and converter. Stone et al. (Stone (1983)) have shown that a significant mismatch can be created by small waveguide gaps less than 2.5λ for higher order circular TE_{0n} modes.

Adding the TE_{02} - to - TE_{01} converter to the end of TE_{03} - to - TE_{02} converter resulted in the far field pattern given in Fig. 5c. The agreement between measurement and theory for a circular TE_{01} mode is better than between theory and experiment for the TE_{02} output from the first converter. This is true despite the poor purity of the TE_{02}

input mode as shown in Fig. 5b. A possible mode mixture at the output of the TE_{02} - to - TE_{01} converter which is in better agreement with the measurement is: 87% TE_{01}, 5% TE_{02}, and 8% TE_{03} with the relative phase of the TE_{02} and TE_{03} modes to the TE_{01} mode of 180° and 35°, respectively. The dashed curve in Fig. 5c gives the theoretical far field pattern for this mode mixture. This mode mixture is not a rigorous fit to the data nor a unique solution, but a best guess approximation. Other reasonable mode combinations tried also indicated a TE_{01} mode purity less than 90%.

A circular TE_{01} mode purity of less than 90% at the output of the TE_{02} - to - TE_{01} converter is much less than the predicted conversion efficiency given in Table I, but in this case most of the disagreement can be attributed to the nonpure circular TE_{02} mode used as input. The interesting observation is that the combined conversion efficiency of these two converters together is better than that of the TE_{03} - to - TE_{02} converter alone. In particular, the fraction of circular TE_{03} mode at the output of the TE_{02} - to - TE_{01} converter has been significantly reduced from that at the input. Numerical solution of Eqs. 16 with an 80%/20%, TE_{02}/TE_{03} mode mixture as input into this converter predicts an 83%/17% TE_{01}/TE_{03} mode mixture at the output, independent of the relative phase between the TE_{02} and TE_{03} modes at the input. No significant TE_{02} component is predicted at the output. Theory therefore supports our observation that the TE_{02} - to - TE_{01} converter will tend to make up for a poorly performing TE_{03} - to - TE_{02} converter, however, the observed level of improvement appears to be

better than predicted. This discrepancy could be attributed to a number of factors including imperfections in the mode converters, slight misalignment between converters, reflections which aren't included in the calculations, or an incorrect estimate of the actual measured mode mixtures from the far field patterns.

The TE_{01} - to - TE_{11} wriggle converter was not available during these tests of the axisymmetric converters and prior to its availability the gyrotron vacuum system was rebuilt. During this time the axisymmetric converters were installed as part of the gyrotron vacuum system. The major advantage of this was to eliminate the 3λ gap and window between the gyrotron output waveguide and TE_{03} - to - TE_{02} converter. A 0.1λ gap was maintained for pumping with another similar gap between the converters. The gyrotron cavity was also changed with the result that the TE_{03} mode frequency was shifted to 136.69 GHz. This small change in frequency should not effect the performance of the converters.

The resulting far field pattern now launched through the vacuum window at the output of the TE_{02} - to - TE_{01} converter is shown in Fig. 6a. There is a distinct asymmetry in the far field pattern which, unfortunately, we believe is due to a very slight bend in the gyrotron output waveguide. However, averaging this asymmetry we can still estimate the relative level of higher order symmetric modes to the TE_{01} mode. The solid curve of Fig. 6a corresponds to a circular TE_{01} mode only, while the solid and dashed curves together correspond to a mode mixture of 92% TE_{01} and 8% TE_{03} with a relative phase of 110°. The

TE_{02} mode appears to be absent. It therefore seems that the elimination of the window and 3λ gap between the gyrotron output guide and TE_{03} - to - TE_{02} converter has not significantly reduced the level of the TE_{03} mode at the output, though the overall purity of the TE_{01} mode in terms of symmetric modes appears to be better.

A 60cm long straight section of 1.27 diameter copper waveguide was butted to the gyrotron vacuum window and the resulting far field pattern is shown in Fig. 6b. This short section of straight waveguide has almost completely filtered out the asymmetry in the TE_{01} output beam. Also, the relative level of higher order symmetric modes has been significantly reduced. The dashed curve in Fig. 6b indicates the level if 3% of the beam was in the TE_{03} mode 180° out of phase with the TE_{01} mode. For the gyrotron diagnostic application there will be over 10m of transmission waveguide between the gyrotron and the TE_{01} - to - TE_{11} wriggle converter. Therefore the mode purity following waveguide transmission is more relevant to the diagnostic application than that at the gyrotron output window.

The cleanup of the TE_{01} beam with the straight waveguide was achieved at the expense of a measurable power loss. The power output from the waveguide was down by $8 \pm 4\%$ as compared to a power measurement directly at the gyrotron output window. The calculated ohmic losses for transmission of the TE_{01} beam through this 60cm long, 1.27cm diameter copper guide is 0.5%, and for the TE_{03} mode 4.2%. An asymmetric mode like the TM_{13} would have a loss of 12.7%. These calculated losses are too small to account for the great improvement in TE_{01} beam purity by this short waveguide. It is possible that some of the filtering may

be due to poorer coupling of the higher order modes into the waveguide at the gyrotron output window.

For the diagnostic application these measured losses will not be a problem and the resulting quality of the TE_{01} beam as given in Fig. 6b is very exceptable for the next stage of conversion.

B. Wriggle Converter

The larger wriggle converter listed in Table II was made by bending thin walled (0.7mm) copper tubing into the desired shape. An aluminum jig was made to facilitate bending this converter into the correct wriggle and then to hold its shape. This jig consisted of a flat plate the length of the converter with a tapped hole at every wriggle peak for holding parts against which the copper tube was bent. These parts could best be described as sectors of a pully. The pully sectors were contoured to fit the outside diameter of the copper tube and the pully radius corresponded to the minimum radius of curvature at the peaks of the sinusoidal wriggle perturbation. Using these pully sectors it was possible to push on the copper tube to achieve the desired wriggle without deforming its circularity. When the desired wriggle was achieved these pully sectors were bolted in place to hold the converter to that shape. The wriggle amplitude could be adjusted experimentally, but the wriggle period was fixed.

The commercially available thin walled copper tubing used for making the TE_{01} - to - TE_{11} wriggle converter had an actual diameter of 1.285cm which required increasing the perturbation period to 13.25cm to keep it centered at a frequency of 137 GHz.

The perturbation amplitude of this converter was optimized experimentally by using this converter in reverse to convert from the TE_{11} to the TE_{01} mode. An Impatt diode was the source of a circular TE_{11} mode by means of a commercially available (Aerowave) rectangular to circular waveguide transition. This was followed by a linear up-taper to 1.27cm diameter waveguide. The E-plane far field pattern at a frequency of 137 GHz launched from this up-taper is shown in Fig. 7a where the points are the measurements and the solid curve is the calculated pattern. Similar good agreement with theory was found for the H-plane.

A compact heterodyne receiver was used for the far field measurements in this case because of the low power levels ($\leq$ 10mW) available from the Impatt diode. The local oscillator for this receiver was a solid state tripled Gunn oscillator from Millitech. This local oscillator along with a Hughes single end mixer, a 3 dB directional coupler as a diplexer, IF amplifiers, and a 0 - 50 dB calibrated attenuator and horn on the receiver front end were all attached to the top of a standard laboratory jack for far field scans. The attenuator was varied as before during the pattern scan to keep the detected signal constant. A 50 dB dynamic range was easily achieved.

Using the circular TE_{11} mode as input to this converter the perturbation amplitude of each wriggle period was adjusted to optimize the far field pattern for a circular TE_{01} mode output. This was particularly easy to do by setting the receiver system on axis at 0°, corresponding to TE_{01} pattern null, and making the adjustments to

minimize the signal here. The resulting TE_{01} pattern is shown in Fig. 7b. There is excellent agreement between theory and measurement. The on-axis null is over 29 dB below the TE_{01} mode peaks. We take this as a measure of the conversion efficiency from the TE_{11} mode which is peaked on axis. The far field pattern in Fig. 7b was taken in the plane perpendicular to the converter wriggle plane which is the same plane which corresponds to the E-plane pattern of Fig. 7a.

These converters are reversable, i.e., conversion from TE_{01} to TE_{11} will be the same as from TE_{11} to TE_{01}. The achieved conversion efficiency of better than 99% is much better than predicted in Table II. The main reason for this is that the perturbation amplitude function down the length of the converter has been adjusted to something more complicated than the linear function assumed for the calculations. Also the wriggle perturbation may not be exactly sinusoidal. It was not possible to determine the perturbation function experimentally achieved because of its smallness.

The Impatt diode and receiver local oscillator used for the converter optimization were tunable so it was possible to check the performance of this converter at other frequencies. Using the ratio of the TE_{01} pattern peak to the on axis minimum as a parameter indicative of the conversion efficiency, we plot this for the frequency range 136.6 to 140.4 GHz in Fig. 8. This ratio gets better at higher frequencies and is about 37 dB at 140 GHz. This shows that the converter is not centered on 137 GHz, which can be accounted for by a perturbation period which is slightly too short. Nevertheless, the conversion

efficiency at 137 GHz is quite satisfactory and is the best reported so far for a converter of this type.

This converter was next used to convert the TE_{01} gyrotron beam. The TE_{01} end of this converter was connected to the output of the waveguide producing the far field pattern given in Fig. 6b. The resulting TE_{11} mode E- and H-plane patterns are shown in Fig. 9.

For these measurements the detection system was always swung in a horizontal arc and the converter wriggle plane was oriented vertical for the E-plane and horizontal for the H-plane scans. In each plane two scans were made, one for each of two orthogonal polarizations. The open circle data in Fig. 9 corresponds to radiation with a polarization 90° relative to the solid circle data. These measurements were made by simply rotating the detection horn 90°.

The agreement of the dominate polarization with the calculated curves is excellent for the E-plane and very good for the H-plane. In the E-plane there is no notable discrepancy down to -30 dB. In the H-plane the main discrepancy is a sidelobe which peaks -15 dB relative to the main peak. This sidelobe seems to correspond approximately to one of the cross polarization sidelobes in the E-plane.

It is difficult to model a mode mixture to reproduce the H-plane measurement. Small additions of higher order TE or TM modes will cause distortions to the far field pattern which are symmetric about the 0° axis. Furthermore it is difficult to find a mode mixture which will not effect the E-plane at the same time. The angular position of the H-plane sidelobe and the E-plane cross polarization sidelobes corresponds approximately to that expected for the peaks of the TE_{02} or the E-plane

TE_{12} mode. In either case their maximum contribution level cannot exceed 3% to agree with the observed levels.

Power measurements at the input and output of this converter revealed no losses within the measurement accuracy of $\pm$ 5%. In fact for the entire converter and waveguide chain, from the input to the TE_{03} - to - TE_{02} converter to the TE_{11} output, the only significant power loss measured was about 8% between the gyrotron output window and wriggle converter. The resulting beam is better than 97% circular TE_{11} mode. This is a very satisfactory result. Further filtering of the beam could be done by optical means after conversion to the HE_{11} mode.

VI. SUMMARY

A unified derivation of the coupled mode equations for deformed circular waveguide has been presented. This derivation presented exact integral relations for the $\underline{E}$ and $\underline{H}$ fields. Several special deformation perturbations were considered. These cases included a varying circular guide diameter, a bend, a noncircular cross section deformation, and finite guide wall conductivity. Each of these waveguide perturbations can lead to mode conversion for a given class of modes.

Optimized converter design requires numerical solution of the coupled mode equations for a sufficiently large collection of modes. However, approximate design criteria were presented considering only the two modes of interest. This served to provide an initial guess of the desired mode converter parameters which could then be optimized by numerical calculations considering competing modes. Using this method we designed a set of mode converters for conversion of a 2mm wave, circular TE_{03} mode in overmode waveguide into the TE_{11} mode.

A pair of axisymmetric mode converters for conversion of the TE_{03} mode first into the TE_{02} and then into TE_{01} mode was found, by numerical calculations, to be more efficient than direct conversion into the TE_{01} mode by a single converter. This was primarily because the beat wavelengths for the mode pairs $TE_{03} - TE_{01}$ and $TE_{03} - TE_{04}$ fall too close together. Also, a waveguide diameter close to 1.27cm seemed optimal in terms of competition from unwanted modes. A calculated conversion efficiency of 99% into the TE_{01} mode was shown.

A TE_{01} - to - TE_{11} wriggle converter was designed with a conversion efficiency of 98%. It was found that a converter length with a nonitegral number of perturbation wavelengths and a perturbation amplitude which was not constant along the length reduced competition from the TE_{12} and TE_{21} modes.

These mode converters were fabricated and then evaluated using a several kilowatt, 137 GHz gyrotron with a very pure TE_{03} mode output. The choice of the diameters of the gyrotron output waveguide and converters was such that no up- or down-tapers were needed. The axisymmetric mode converters did not initially achieve the predicted conversion efficiencies. In particular, the TE_{03} - to - TE_{02} converter was only 80% effective. The TE_{02} - to - TE_{01} converter was found to partially make up for the poor performance of the TE_{03} - to - TE_{02} converter with a resulting TE_{01} mode purity of approximatley 87%.

It was suspected that part of the reason for the poor performance was the 3λ gap due to the vacuum window between the gyrotron output waveguide and mode converters. The gyrotron vacuum system was subsequently rebuilt with the axisymmetric mode converters in the vacuum and the gap between output waveguide and mode converters reduced to 0.1λ. The output purity of the TE_{01} mode with respect to higher order axisymmetric modes was improved to 92%. Further improvement to 97% TE_{01} mode purity was achieved with a short section of straight waveguide butted to the vacuum window. It seems that the higher order modes were more poorly coupled through the window gap to the waveguide than the TE_{01} mode. An approximately 8% power loss was also measured at this point.

The TE_{01} - to - TE_{11} wriggle converter was made by bending a thin walled copper waveguide to shape. The perturbation amplitude was adjusted experimentally for a conversion efficiency of better than 99% not including ohmic losses. This is the best result reported for this type of converter to date.

Using this wriggle converter at the output of the waveguide with a 97% pure TE_{01} gyrotron beam resulted in an approximatley 97% pure TE_{11} beam. This kind of TE_{11} beam purity with a measured power loss of only 8% for the entire converter chain (with a vacuum window and short waveguide between the axisymmetric and wriggle converters) is a very good result.

Appendix A.

Circular waveguide modes.

Harmonically varying wavemode solutions in the straight circular wave guide with perfectly conducting wall (referred to as the ideal guide in this text) are called TM (or E) - waves or TE (or H) - waves, satisfying $H_z = 0$ and $E_z = 0$ respectively. Two indices m,n are required to specify each mode uniquely. In addition most modes ($m > 0$) has a two-fold polarization degeneracy. For convenience, these indices and the polarization indicator will sometimes be represented by a single index s or even referred to without any index. Indices will be included in parenthesis or brackets where necessary to specify TM - or TE - modes. Thus $\underline{E}_{(mn)}$ and $\underline{E}_{[mn]}$ indicate the electric fields of the TM_{mn} - and TE_{mn} - modes, respectively.

The transverse electric and magnetic fields are given as

$$\underline{E} = V(z)\, \underline{e} \tag{A.1}$$

$$\underline{H} = I(z)\, \underline{h}$$

where

$$\underline{h} = \hat{\underline{z}} \times \underline{e} \qquad \underline{e} = \underline{h} \times \hat{\underline{z}}. \tag{A.2}$$

For TM - waves

$$\underline{e}_{mn} = -\nabla \Phi_{mn}(r,\phi) \qquad (A.3)$$

$$\Phi_{mn} = -C_{mn} J_m(p_{mn} r) \begin{Bmatrix} \cos m\phi \\ \sin m\phi \end{Bmatrix}$$

where

$$C_{mn} = \frac{\theta_m}{\sqrt{\pi}\, \chi_{mn} J'_m(\chi_{mn})}$$

and

$$J_m(\chi_{mn}) = 0 .$$

Here $\theta_m = 1$ for $m = 0$, $\theta_m = \sqrt{2}$ for $m > 0$, $\chi_{mn} = a p_{mn}$ and J_m is the Bessel function of first kind and order m. In particular

$$\underline{e}_{mn} = C_{mn} \left(\hat{\underline{r}}\, p_{mn} J'_m(p_{mn} r) \begin{Bmatrix} \cos m\phi \\ \sin m\phi \end{Bmatrix} + \hat{\underline{\phi}} \frac{m}{r} J_m(p_{mn} r) \begin{Bmatrix} -\sin m\phi \\ \cos m\phi \end{Bmatrix} \right) \qquad (A.4)$$

$$\underline{h}_{mn} = C_{mn} \left(\hat{\underline{r}}\, \frac{m}{r} J_m(p_{mn} r) \begin{Bmatrix} \sin m\phi \\ -\cos m\phi \end{Bmatrix} + \hat{\underline{\phi}}\, p_{mn} J'_m(p_{mn} r) \begin{Bmatrix} \cos m\phi \\ \sin m\phi \end{Bmatrix} \right).$$

In addition

$$E_z = \frac{p^2}{j\omega\epsilon} I \Phi \qquad (A.5)$$

$$\frac{dV}{dz} + (j\omega\mu + \frac{p^2}{j\omega\epsilon})I = 0$$

$$\frac{dI}{dz} + j\omega\epsilon V = 0 \; . \qquad (A.6)$$

The choice of the sine or cosine function in the Φ-expression determines the polarization of the mode. With the cosine function (the upper choice) the electric field near the axis of the guide will be polarized parallel to the $\phi = 0$ plane for $m > 0$ modes.

For TE - waves the corresponding formulas are

$$\underline{h}_{mn} = - \nabla \Phi_{mn} (r,\phi)$$

$$\Phi_{mn} = - C_{mn} J_m (p_{mn} r) \begin{Bmatrix} \sin m\phi \\ -\cos m\phi \end{Bmatrix} \qquad (A.7)$$

this time with

$$C_{mn} = \frac{\theta_m}{\sqrt{\pi}\,(\chi_{mn}^2 - m^2)^{1/2} \; J_m(\chi_{mn})}$$

and

$$J_m' (\chi_{mn}) = 0 \; .$$

Therefore

$$\underline{e}_{mn} = C_{mn}\left(\hat{\underline{r}}\,\frac{m}{r}\,J_m(p_{mn}r)\begin{Bmatrix}\cos m\phi\\ \sin m\phi\end{Bmatrix} + \hat{\underline{\phi}}\,p_{mn}\,J'_m(p_{mn}r)\begin{Bmatrix}-\sin m\phi\\ \cos m\phi\end{Bmatrix}\right)$$

(A.8)

$$\underline{h}_{mn} = C_{mn}\left(\hat{\underline{r}}\,p_{mn}\,J'_m(p_{mn}r)\begin{Bmatrix}\sin m\phi\\ -\cos m\phi\end{Bmatrix} + \hat{\underline{\phi}}\,\frac{m}{r}\,J_m(p_{mn}r)\begin{Bmatrix}\cos m\phi\\ \sin m\phi\end{Bmatrix}\right)$$

and finally

$$H_z = \frac{p^2}{j\omega\mu}\,V\,\phi \qquad \text{(A.9)}$$

$$\frac{dV}{dz} + j\omega\mu\, I = 0$$

$$\frac{dI}{dz} + \left(j\omega\epsilon + \frac{p^2}{j\omega\mu}\right) V = 0 \qquad \text{(A.10)}$$

With the sine function choice (the upper choice) in the Φ-expression the electric field near the axis of the guide will again be polarized parallel to the $\phi = 0$ plane for $m > 0$ modes.

We note that for both types of modes

$$\nabla^2 \Phi(r,\phi) + p^2 \Phi(r,\phi) = 0 \qquad \text{(A.11)}$$

The normalization constants C_{mn} which take alternate signs with increasing second index n, have been chosen so that

$$\int dS\, \underline{e}_s \cdot \underline{e}_{s'} = \int dS\, \underline{h}_s \cdot \underline{h}_{s'} = p^2 \int dS \Phi^2 = 1. \qquad \text{(A.12)}$$

All modes are mutually orthogonal, that is for $s' \neq s$

$$\int dS\, \underline{e}_s \cdot \underline{e}_{s'} = \int dS\, \underline{h}_s \cdot \underline{h}_{s'} = \int dS \Phi_s \Phi_{s'} = 0 \qquad \text{(A.13)}$$

For both types of modes the solution of the generalized telegraphist equations (A6) and (A10) can be written in the form

$$V(z) = \sqrt{Z}\,(Ae^{-\gamma z} + Re^{\gamma z})$$

$$I(z) = \frac{1}{\sqrt{Z}}\,(Ae^{-\gamma z} - Re^{\gamma z}) \qquad \text{(A.14)}$$

where the propagation constant γ and the wave impedance Z are given by

$$\gamma^2 = p^2 - \omega^2 \varepsilon \mu$$

$$Z = \sqrt{\frac{\mu}{\epsilon}} \begin{cases} \frac{j\omega\sqrt{\epsilon\mu}}{\gamma} & \text{for TE - modes} \\ \\ \frac{\gamma}{j\omega\sqrt{\epsilon\mu}} & \text{for TM - modes} \end{cases} \qquad \text{(A.15)}$$

For propagating modes, $\gamma^2 < 0$, we note that $\gamma = j\sqrt{|\gamma^2|} \equiv j\beta$. The power in a particular forward propagating mode is given by the absolute square of the amplitude A.

TABLE I

AXISYMMETRIC MODE CONVERTERS

	$TE_{03} \rightarrow TE_{02}$	$TE_{02} \rightarrow TE_{01}$
AVERAGE DIAMETER, $2a$	1.225 cm	1.194 cm
DIAMETER VARIATION, ν	± 3.7%	± 6.4%
BEAT WAVELENGTH, L	2.148 cm	3.500 cm
NUMBER OF BEATS, N	5	5
TOTAL LENGTH, l	10.740cm	17.500 cm
CONVERSION EFF. (CALCULATED)	99.0%	99.8%

TABLE II

$TE_{01} \rightarrow TE_{11}$ CONVERTERS

WAVEGUIDE DIAMETER, $2a$	1.27 cm	0.800 cm
WRIGGLE AMPLITUDE, ν	4.1 → 8.5%	6.2 → 9.6%
BEAT WAVELENGTH, L	12.90 cm	5.04 cm
NUMBER OF BEATS, N	7.75	6.25
TOTAL LENGTH, l	99.98 cm	31.50 cm
CONVERSION EFF. (CALCULATED)	97.9%	96.9%

FIGURE CAPTIONS

1. Illustration of the axisymmetric (a) and wriggle (b) converter perturbations. The vertical scale is greatly exaggerated.

2. Calculated performance of the optimized TE_{03} - to - TE_{02} converter; (a) conversion of power from the TE_{03} mode at 137 GHz as the beam propagates down the converter length; (b) converter performance as a function of frequency.

3. Calculated performance of the optimized TE_{02} - to - TE_{01} converter; (a) conversion of power from the TE_{02} mode at 137 GHz as the beam propagates down the converter length; (b) converter performance as a function of frequency.

4. Calculated performance of the 1.27cm diameter TE_{01} - to - TE_{11} converter; (a) conversion of power from the TE_{01} mode as the beam propagates down the converter length; (b) converter performance as a function of frequency.

5. Calculated (lines) and measured (points) far field patterns; (a) from gyrotron output window, (b) from TE_{03} - to - TE_{02} converter butted to gyrotron window, (c) from TE_{02} - to - TE_{01} converter butted to output of TE_{03} - to - TE_{02} converter in (b).

6. Calculated (lines) and measured (points) far field patterns; (a) from gyrotron output window with axisymmetric TE_{03} - to - TE_{02} and TE_{02} - to - TE_{01} converters installed inside vacuum, (b) after propagation through 60cm long, 1.27 cm diameter copper waveguide butted to vacuum window. The higher order calculated peaks of a pure TE_{01} mode have not been included in this figure. See Fig. 7a.

7. Calculated (lines) and measured (points) far field patterns at 137 GHz; (a) from Impatt diode with rectangular to circular waveguide transition followed by 7° linear up-taper to 1.27 diameter aperture, (b) from TE_{01} - to - TE_{11} wriggle converter connected in reverse to output from up-taper used in (a). Wriggle converter perturbation amplitude was experimentally optimized to minimize TE_{01} mode null on axis to better than -29 dB.

8. Measured TE_{01} - to - TE_{11} converter performance as a function of frequency. Ratio of TE_{01} mode far field pattern peak to on-axis null is plotted as a function of frequency. Conversion efficiency seems to peak near 140 GHz with an efficiency of 99.98%.

9. Calculated (lines) and measured (points) far field patterns from the TE_{01} - to - TE_{11} converted butted to the gyrotron waveguide giving the far field pattern in Fig. 6(b). Open points correspond to a polarization 90° relative to the solid points (a) E-plane, (b) H-plane.

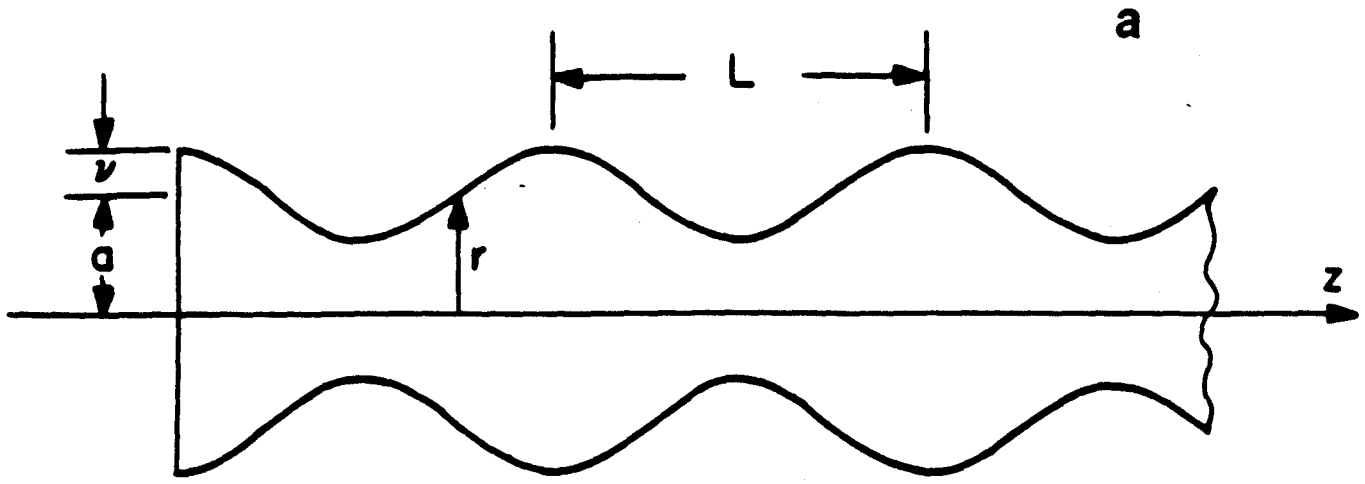

AXISYMMETRIC $TE_{on} \rightarrow TE_{on'}$ CONVERTER

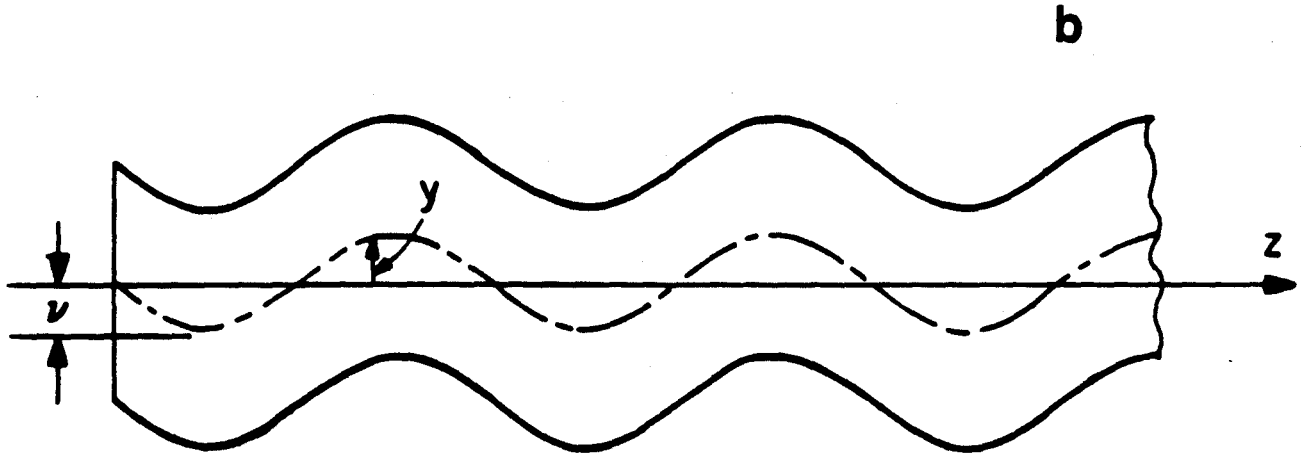

WRIGGLE $TE_{01} \rightarrow TE_{11}$ CONVERTER

Fig. 1

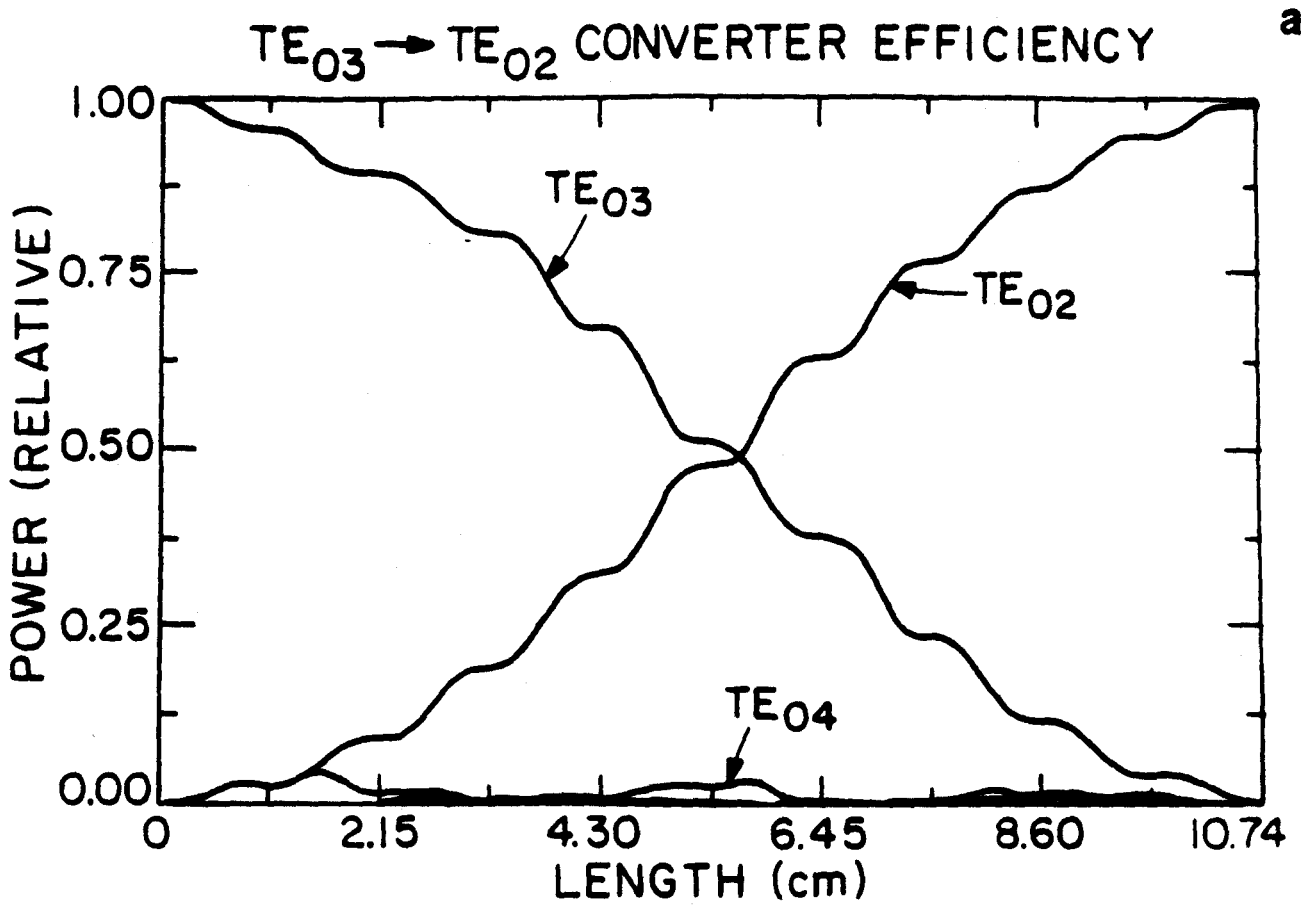
a
TE03 → TE02 CONVERTER EFFICIENCY
1.00
0.75
0.50
0.25
0.00
POWER (RELATIVE)
TE03
TE02
TE04
0
2.15
4.30
6.45
8.60
10.74
LENGTH (cm)

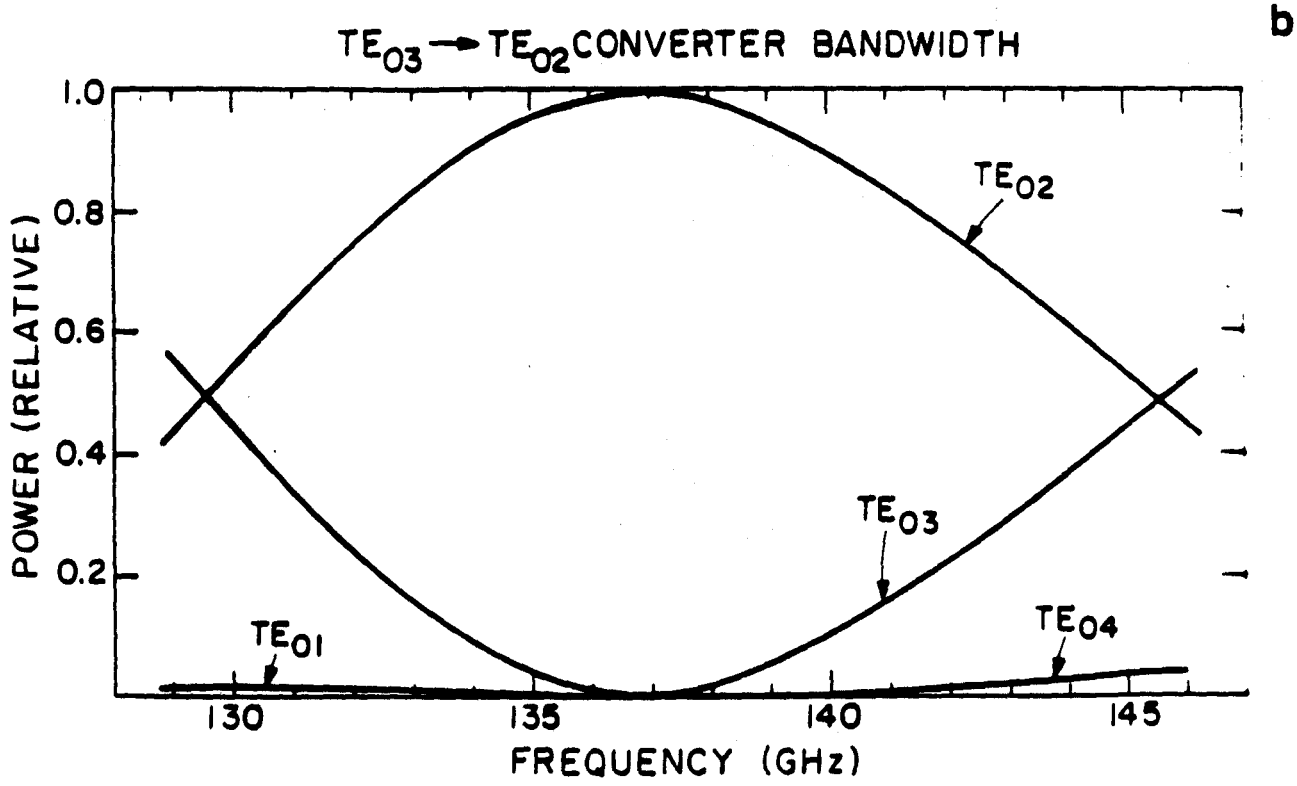
b
TE03 → TE02 CONVERTER BANDWIDTH
1.0
0.8
0.6
0.4
0.2
POWER (RELATIVE)
TE02
TE03
TE01
TE04
130
135
140
145
FREQUENCY (GHz)

Fig. 2

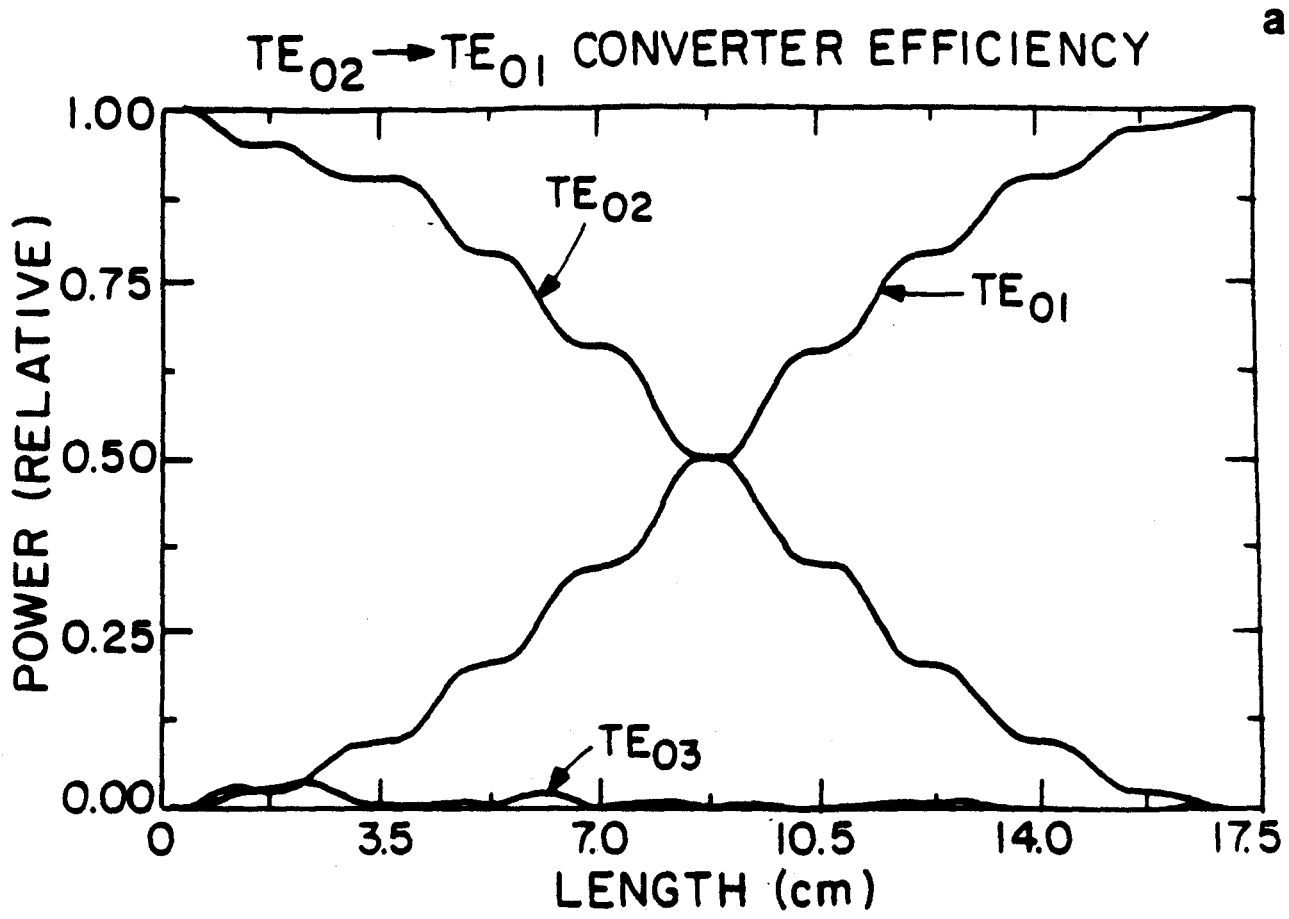
a
TE02 → TE01 CONVERTER EFFICIENCY
1.00
0.75
0.50
0.25
0.00
POWER (RELATIVE)
TE02
TE01
TE03
0
3.5
7.0
10.5
14.0
17.5
LENGTH (cm)

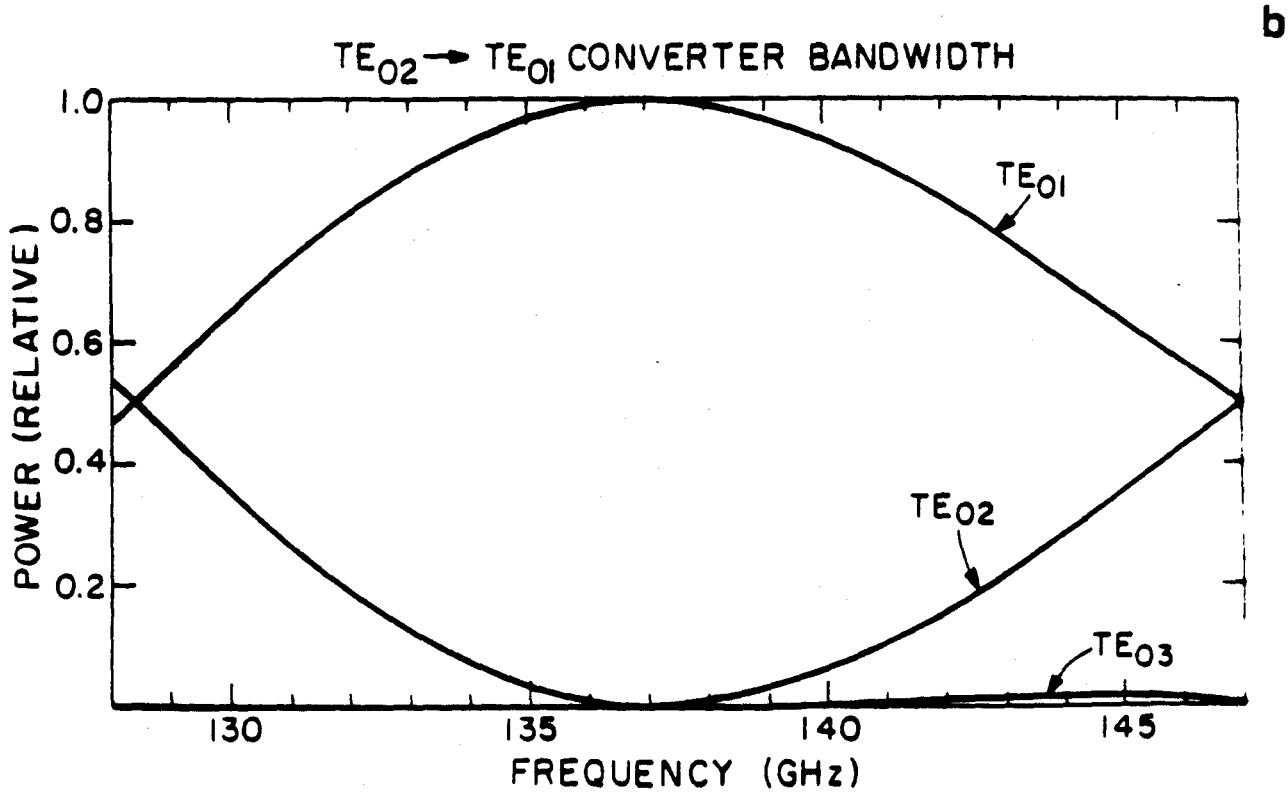
b
TE02 → TE01 CONVERTER BANDWIDTH
1.0
0.8
0.6
0.4
0.2
POWER (RELATIVE)
TE01
TE02
TE03
130
135
140
145
FREQUENCY (GHz)

Fig. 3

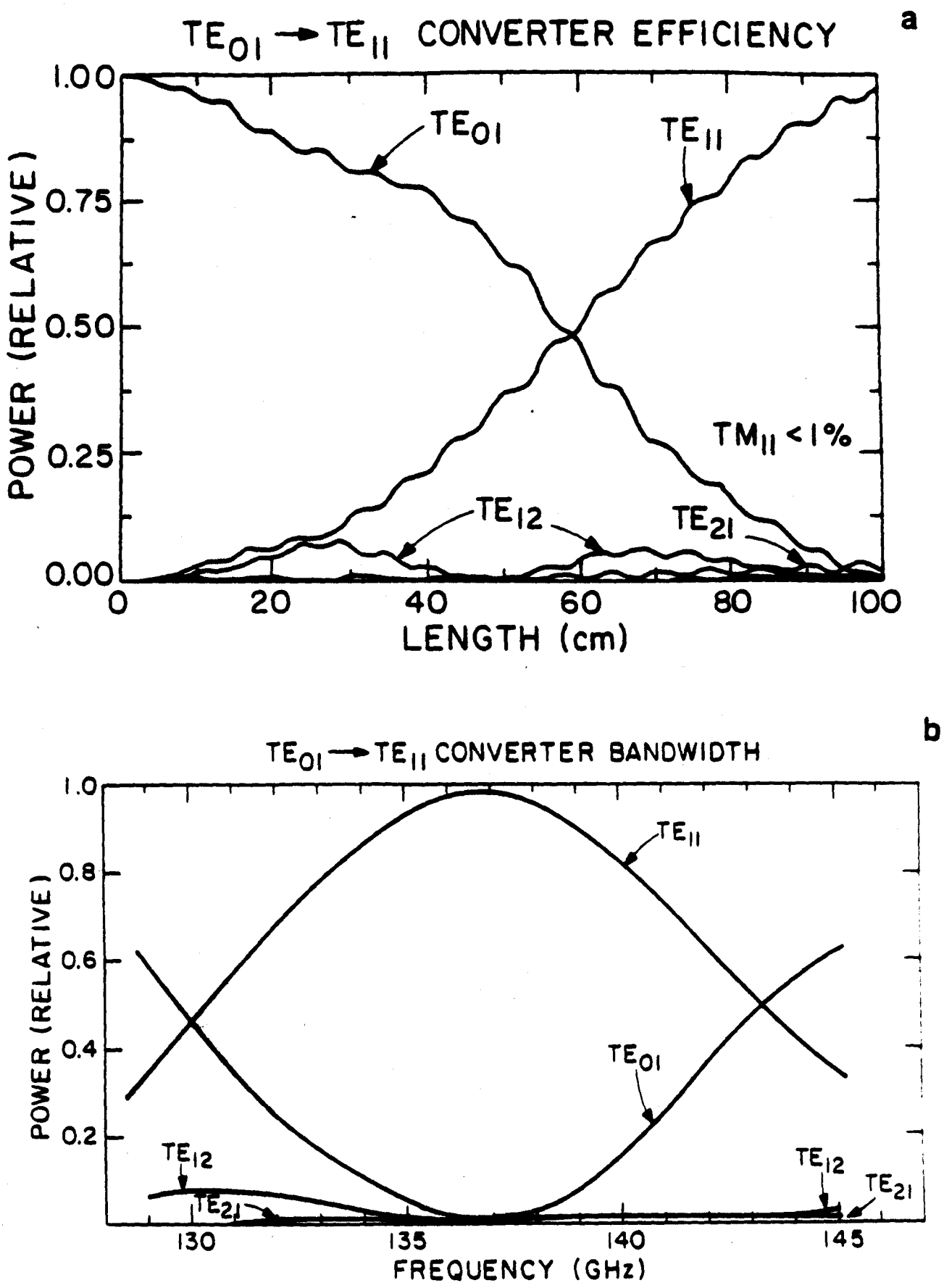
a
TE01 → TE11 CONVERTER EFFICIENCY
1.00
0.75
0.50
0.25
0.00
POWER (RELATIVE)
TE01
TE11
TM11 < 1%
TE12
TE21
0
20
40
60
80
100
LENGTH (cm)
b
TE01 → TE11 CONVERTER BANDWIDTH
1.0
0.8
0.6
0.4
0.2
POWER (RELATIVE)
TE11
TE01
TE12
TE21
TE12
TE21
130
135
140
145
FREQUENCY (GHz)

Fig. 4

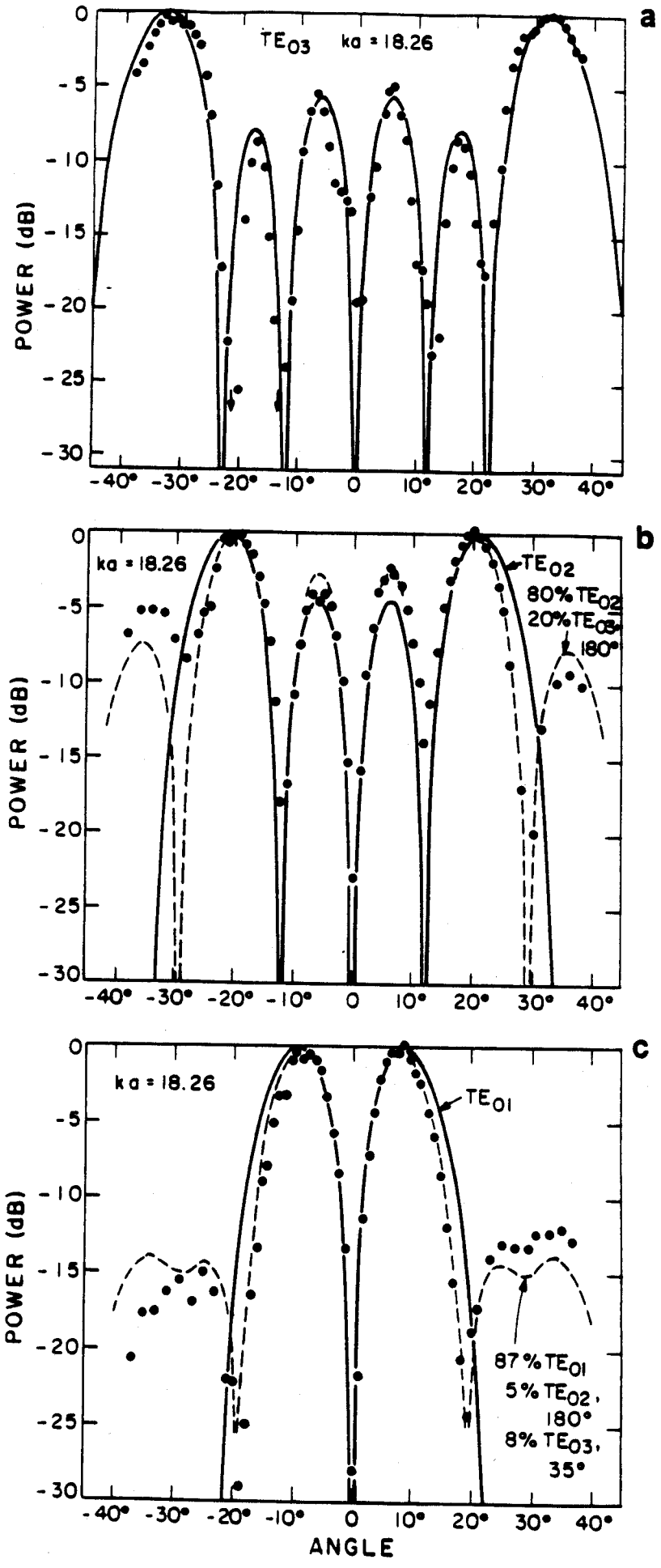
a
TE03 ka = 18.26
POWER (dB)
0
-5
-10
-15
-20
-25
-30
-40° -30° -20° -10° 0 10° 20° 30° 40°
b
ka = 18.26
TE02
80% TE02
20% TE03, 180°
POWER (dB)
c
ka = 18.26
TE01
87% TE01
5% TE02, 180°
8% TE03, 35°
POWER (dB)
ANGLE

Fig. 5

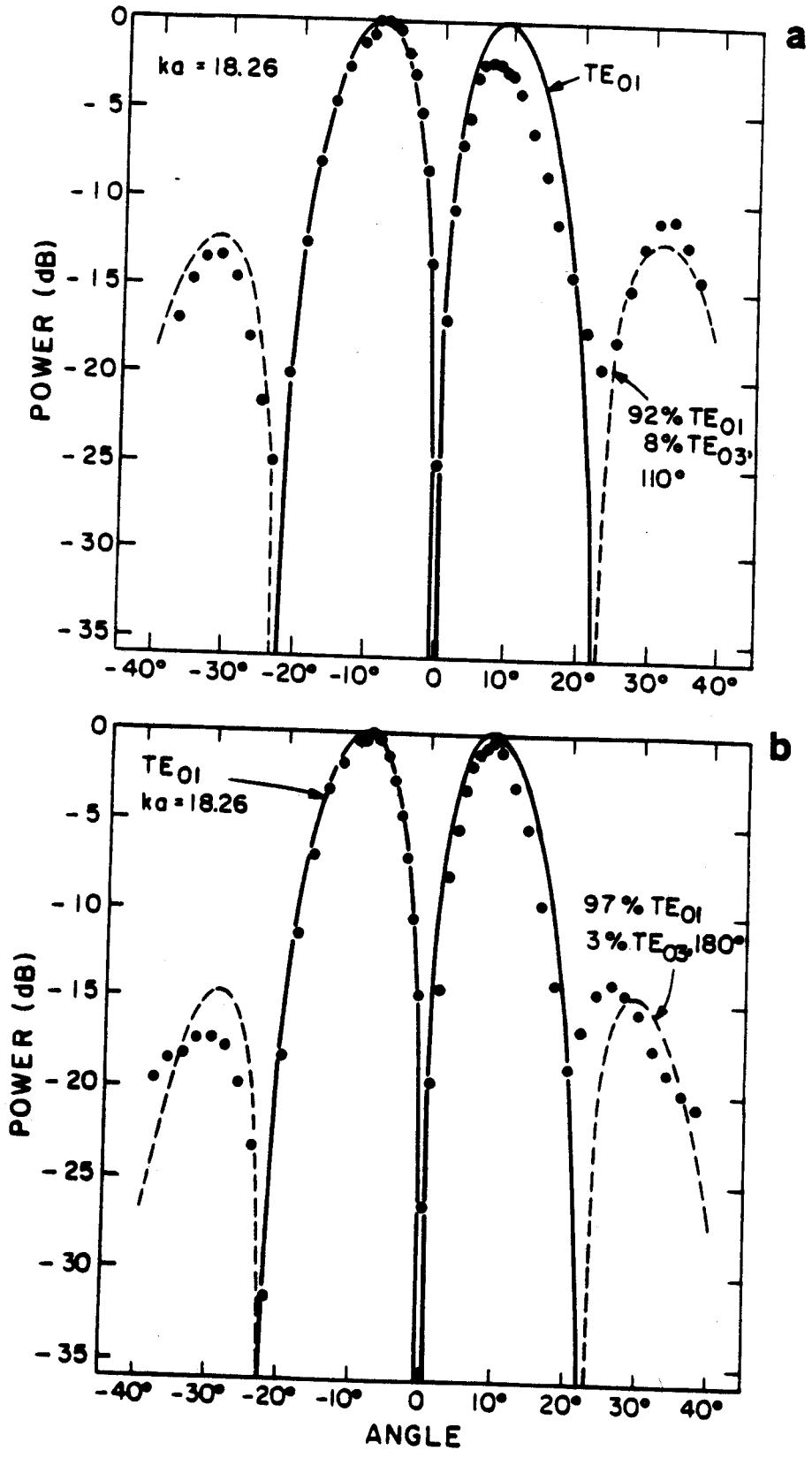
a
ka = 18.26
TE01
92% TE01
8% TE03
110°
POWER (dB)
0
-5
-10
-15
-20
-25
-30
-35
-40° -30° -20° -10° 0 10° 20° 30° 40°
b
TE01
ka = 18.26
97% TE01
3% TE03, 180°
POWER (dB)
ANGLE

Fig. 6

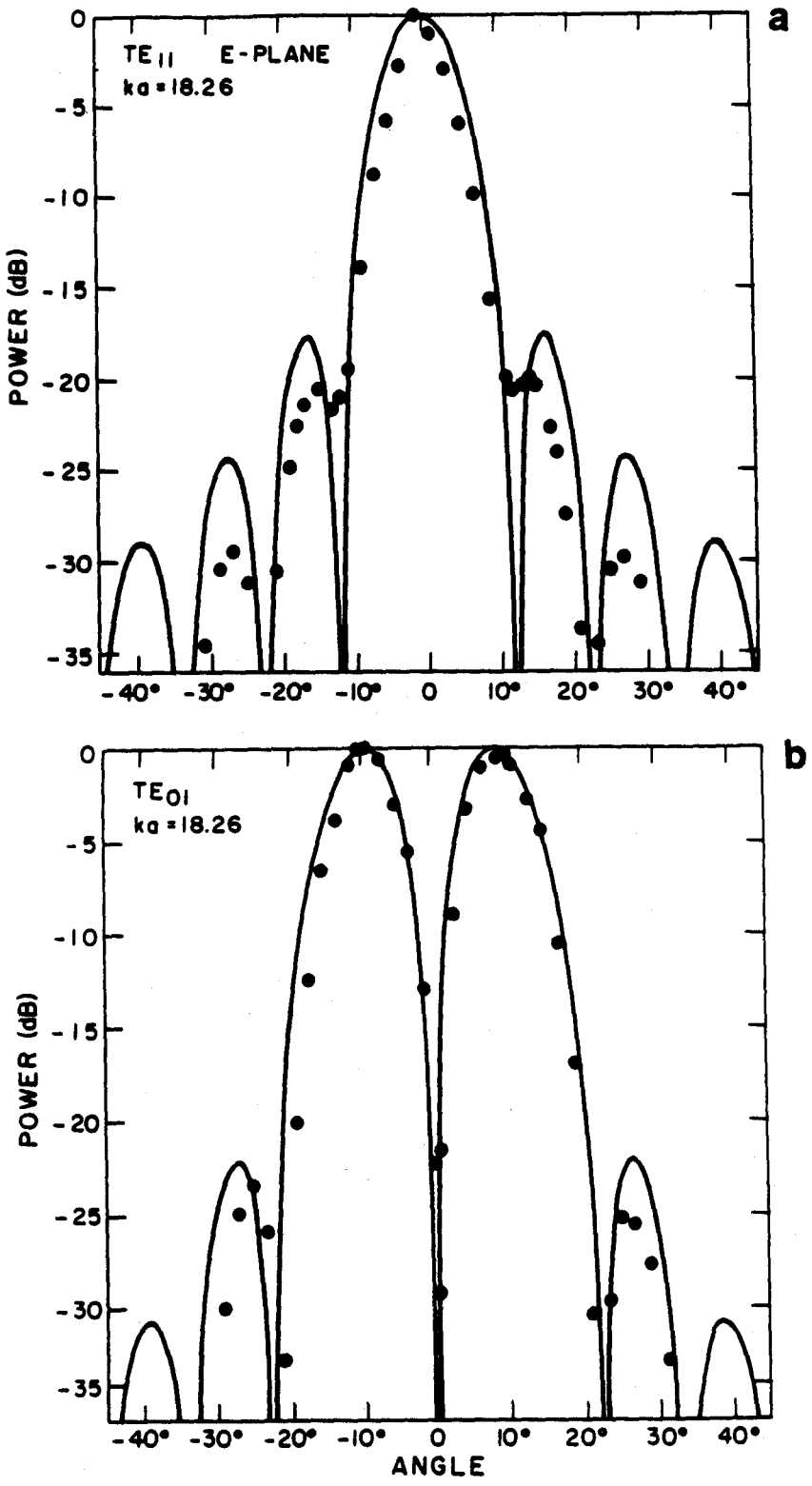
a
TE11 E-PLANE
ka = 18.26
POWER (dB)
0
-5
-10
-15
-20
-25
-30
-35
-40° -30° -20° -10° 0 10° 20° 30° 40°
b
TE01
ka = 18.26
POWER (dB)
ANGLE

Fig. 7

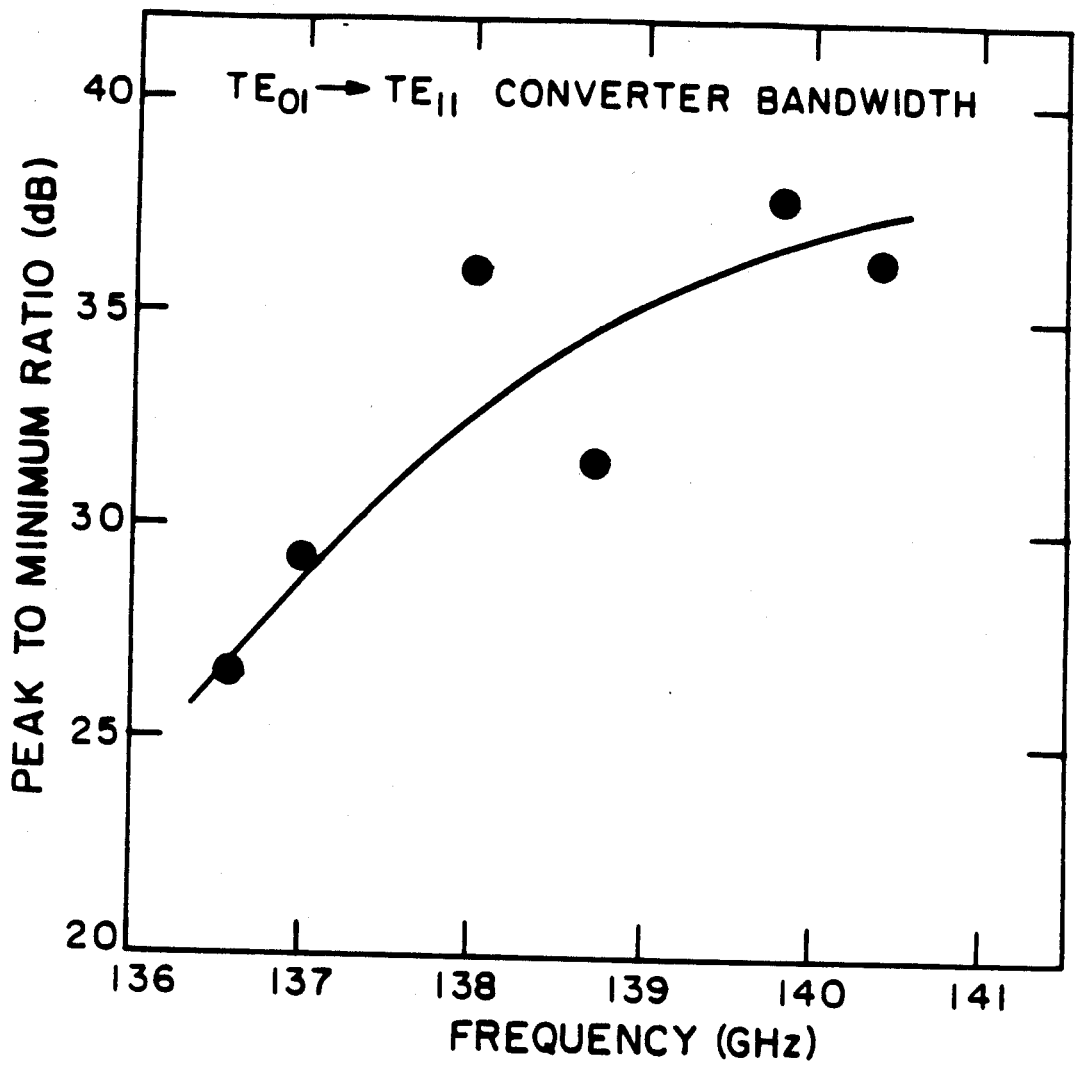
TE01 → TE11 CONVERTER BANDWIDTH
PEAK TO MINIMUM RATIO (dB)
40
35
30
25
20
136
137
138
139
140
141
FREQUENCY (GHz)

Fig. 8

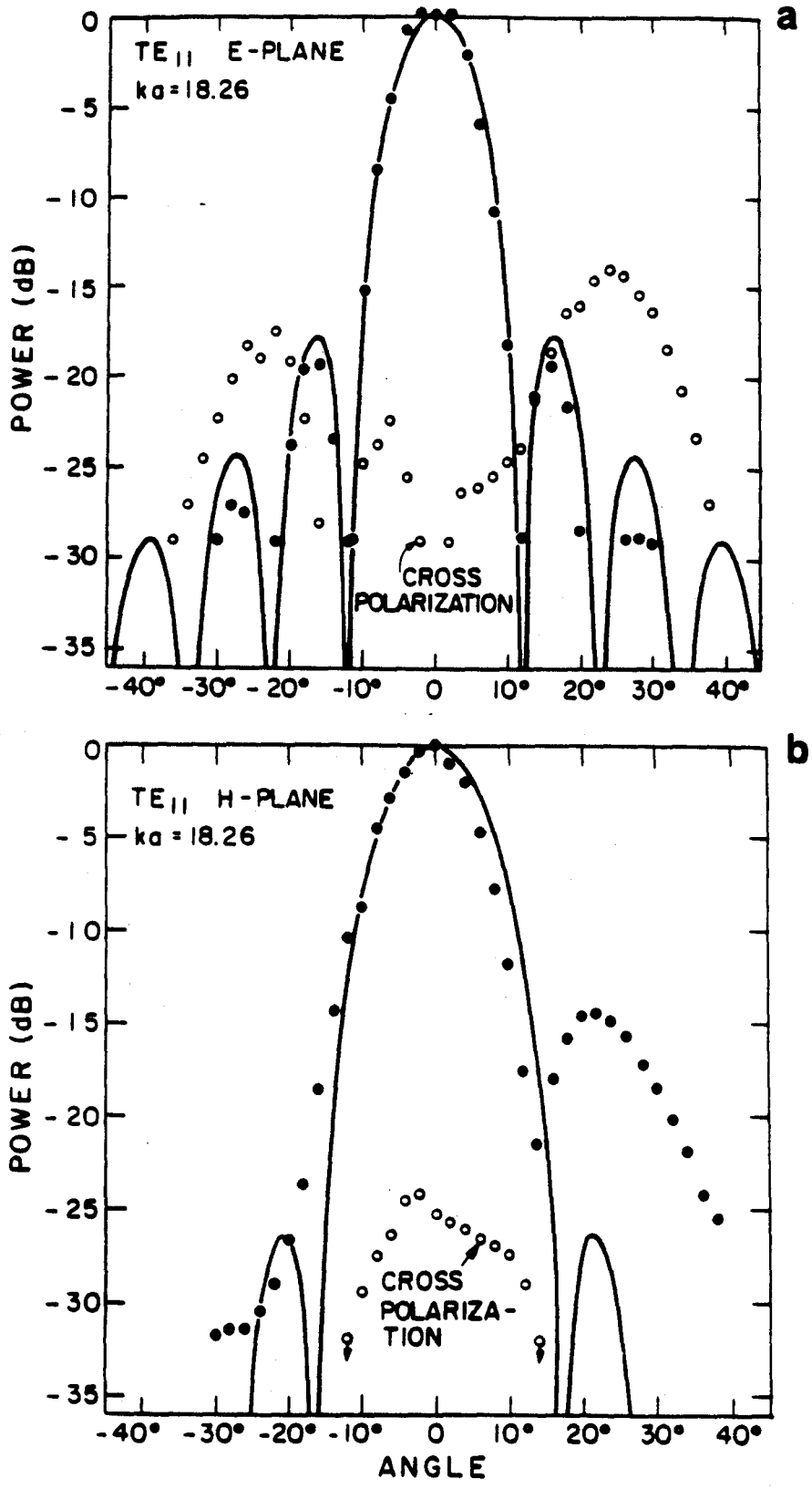
a
TE11 E-PLANE
ka=18.26
POWER (dB)
0
-5
-10
-15
-20
-25
-30
-35
CROSS POLARIZATION
-40° -30° -20° -10° 0 10° 20° 30° 40°
b
TE11 H-PLANE
ka = 18.26
POWER (dB)
CROSS POLARIZA-TION
ANGLE

Fig. 9

References

1. R. E. Collin, Foundations for Microwave Engineering, McGraw-Hill (1966).

2. J. L. Doane, Mode Converters for Generating the HE_{11} (Gaussian-Like) Mode from TE_{01} in Circular Waveguide, Int. J. Electronics 53, 573 (1982).

3. J. L. Doane, Infrared and Millimeter Waves, Vol 13, Ed. by K. J. Button, Academic Press, Inc., Orlando, Chapter 5 (1985).

4. N. C. Gallagher, Jr. and D. W. Sweeney, Microwave Kinoform for Magnetic Fusion, LLNL Report UCPL-89603 (1983).

5. G. L. James, Analysis and Design of TE_{11} - to - HE_{11} Corrugated Cylindrical Waveguide Mode Converters, IEEE Trans. on Microwave Theory and Tech., MTT-29, 1059 (1981).

6. K. E. Kreischer, J. B. Schutkeker, B. G. Danly, W. J. Mulligan, and R. J. Temkin, High Efficiency Operation of a 140 GHz Pulsed Gyrotron, Int. J. Electronics 57, 835 (1984).

7. S. E. Miller, Coupled Wave Theory and Waveguide Applications, Bell System Tech. J. 33, 667 (1954).

8. C. Moeller, Mode converters used in the Doublet III ECH Microwave System, Int. J. Electronics 53, 587 (1982).

9. S. P. Morgan, Theory of Curved Circular Waveguide Containing an Inhomogeneous Dielectric, Bell Syst. Tech. J. 36, 1209 (1957).

10. H. E. Rowe and W. P. Warters, Transmission in Multimode Waveguide with Random Imperfections, Bell Syst. Tech. J. 41, 1031, (1962).

11. M. Thumm, V. Erckmann, G. Janzen, G. Muller, P. G. Schuller, and R. Wilhelm, ECRH Systems for Linearly Polarized Plasma Irradiation in the HE_{11} mode at 28 and 70 GHz, Fourth Int. Symp. on Heating in Toroidal Plasmas, Rome, 21-28 March, (1984).

12. M. Thumm, Computer-Aided Analysis and Design of Corrugated TE_{11} to HE_{11} Mode Converters in Highly Overmoded Waveguides, Int. J. of IR and MM Waves, 6, 577, (1985).

13. S. H. Schelkunoff, Conversion of Maxwell's Equations into Generalized Telegraphist Equations, Bell Syst. Tech. J. 34, 995 (1955).

14. S. Silver, Microwave Antenna Theory and Design, McGraw-Hill Book Co., Inc., New York, Chapter 10 (1949).

15. D. S. Stone, K. L. Felch, and S. T. Sprang, Mode-Specific Reflectometry in a Multimode Waveguide, IEEE Trans. on Microwave Theory and Tech., MTT-31, 710 (1983).

16. H. G. Unger, Circular Waveguide Taper of Improved Design, Bell Syst. Tech. J. 37, 899 (1958).

17. S. N. Vlasov and I. M. Orlova, Quasioptical Transformer which Transforms the Waves in a Waveguide having a Circular Cross Section into a Highly Directional Wave Beam, Izvestiya Vysshikh Uchebnykh Zavedenii, Radiofizika, 15, 148 (1974).

18. R. D. Wengenroth, A Mode Transducing Antenna, IEEE Trans. on Microwave Theory and Tech., MTT-26, 332 (1978).